SIAM J. CONTROL OPTIM.
Vol. 54, No. 3, pp. 1558–1584

SHARP INTERFACE LIMIT FOR A PHASE FIELD MODEL IN STRUCTURAL OPTIMIZATION*

LUISE BLANK†, HARALD GARCKE†, CLAUDIA HECHT†, AND CHRISTOPH RUPPRECHT†

Abstract. We formulate a general shape and topology optimization problem in structural optimization by using a phase field approach. This problem is considered in view of well-posedness, and we derive optimality conditions with minimal regularity assumptions. We relate the diffuse interface problem to a perimeter penalized sharp interface shape optimization problem in the sense of Γ-convergence of the reduced objective functional. Additionally, the convergence of the equations of the first variation can be shown. The limit equations can also be derived directly from the problem in the sharp interface setting. Numerical computations demonstrate that the approach can be applied for complex structural optimization problems.

Key words. shape and topology optimization, linear elasticity, sensitivity analysis, optimality conditions, Γ-convergence, phase field method, diffuse interface, numerical simulations

AMS subject classifications. 35Q74, 35R35, 49Q10, 49Q12, 74B05, 74Pxx

DOI. 10.1137/140989066

1. Introduction.

In structural optimization one tries to find an optimal material configuration of two different elastic materials in some fixed container, where optimal means that a certain objective functional depending on the behavior of the elastic materials is minimized. The control here is represented by the material distribution. Applications of shape and topology optimization span from crash-worthiness of transport vehicles and tunnel design to biomechanical applications such as bone remodeling. Structural optimization has turned out to be helpful in solving automotive design problems in order to maximize the stiffness of vehicles or to reduce the stresses to improve durability; see, for instance, [9].

One of the first approaches for finding the optimal material distribution in the presence of two materials can be found in [43]. However the problem of finding optimal structures in mechanical engineering dates at least back to the beginning of the 20th century when Michell [34] considered optimal truss layouts. It has turned out that generally those problems are not well-posed, because oscillations occur on a very fine scale, see, for example [8], and hence several ideas have been developed to overcome this issue. One important contribution is certainly the idea of using a perimeter penalization in optimal shape design and considering this problem in the framework of Caccioppoli sets, see [5], in order to prevent the abovementioned oscillations. Additionally, it turns out that it is difficult to control the state variables if they are only given on varying domains of definitions. And therefore a so-called ersatz material approach has been introduced; see, for instance, [2, 17]. Here, one replaces the void regions by an ersatz material which may have a very low stiffness. We also remark that there appear many problems of practical relevance where one wants to fill a given domain with two different materials (and not a single material and void)

*Received by the editors September 26, 2014; accepted for publication (in revised form) March 25, 2016; published electronically June 9, 2016.
http://www.siam.org/journals/sicon/54-3/98906.html

†Fakultät für Mathematik, Universität Regensburg, 93040 Regensburg, Germany (Luise.Blank@mathematik.uni-regensburg.de, Harald.Garcke@mathematik.uni-regensburg.de, Claudia.Hecht@mathematik.uni-regensburg.de, Christoph.Rupprecht@mathematik.uni-regensburg.de).

such that after an applied load an objective functional is minimized. Having this in mind it is the main goal of this paper to analyze and numerically solve problems with two materials, whether one is an ersatz material or not.

We start by stating a perimeter penalized shape optimization problem with a general objective functional in section 2.2. This is in a simplified form given as

$$\begin{aligned}&\min_{(\varphi,\boldsymbol{u})} J_0(\varphi,\boldsymbol{u}) := \int_\Omega h_\Omega(x,\boldsymbol{u})\,\mathrm{d}x + \int_{\Gamma_g} h_\Gamma(s,\boldsymbol{u})\,\mathrm{d}s + \gamma c_0 P_\Omega(\{\varphi=1\})\\ &\text{subject to } \int_\Omega \mathcal{C}(\varphi)\left(\mathcal{E}(\boldsymbol{u}) - \overline{\mathcal{E}}(\varphi)\right) : \mathcal{E}(\boldsymbol{v})\,\mathrm{d}x\\ &\qquad = \int_\Omega \boldsymbol{f}\cdot\boldsymbol{v}\,\mathrm{d}x + \int_{\Gamma_g} \boldsymbol{g}\cdot\boldsymbol{v}\,\mathrm{d}s \quad \forall \boldsymbol{v}\end{aligned} \tag{1}$$

and $\varphi \in \{\pm 1\}$. The last term of J_0 represents the perimeter penalization, i.e., the perimeter of the region $P_\Omega(\{\varphi = 1\})$ multiplied by some weighting factor γ and a technical constant c_0. The first two terms in J_0 are volume and surface functions involving the displacement $\boldsymbol{u}$ which describe mechanical expressions to be minimized, and the state equations are a weak form of the equations of linearized elasticity. For details on this equations we refer to section 2.2.

After showing well-posedness we derive necessary optimality conditions by geometric variations without any additional regularity assumption on the minimizing set other than being a Caccioppoli set. This seems to be new as classical shape derivatives always assume at least an open Lipschitz domain as minimizer, see [1, 3, 4, 42] or for simpler systems [11, 32, 33, 37], and they do not treat a general objective functional. We also show that the obtained conditions are consistent with existing results obtained with shape derivatives if the minimizing shape inherits a certain regularity. Then we approximate this problem by using a phase field approach where the free boundary is replaced by a diffuse interface with small thickness related to a parameter $\varepsilon > 0$. Hence, as in [17], the perimeter functional is replaced by the Ginzburg–Landau energy and the optimization problemsection (1) reads as (cf. section 2.3)

$$\begin{aligned}&\min_{(\varphi,\boldsymbol{u})} J_\varepsilon(\varphi,\boldsymbol{u}) := \int_\Omega h_\Omega(x,\boldsymbol{u})\,\mathrm{d}x + \int_{\Gamma_g} h_\Gamma(s,\boldsymbol{u})\,\mathrm{d}s + \gamma\int_\Omega \frac{\varepsilon}{2}\left|\nabla\varphi\right|^2 + \frac{1}{\varepsilon}\psi(\varphi)\,\mathrm{d}x\\ &\text{subject to } \int_\Omega \mathcal{C}(\varphi)\left(\mathcal{E}(\boldsymbol{u}) - \overline{\mathcal{E}}(\varphi)\right) : \mathcal{E}(\boldsymbol{v})\,\mathrm{d}x\\ &\qquad = \int_\Omega \boldsymbol{f}\cdot\boldsymbol{v}\,\mathrm{d}x + \int_{\Gamma_g} \boldsymbol{g}\cdot\boldsymbol{v}\,\mathrm{d}s \quad \forall \boldsymbol{v}.\end{aligned} \tag{2}$$

After discussing well-posedness and necessary optimality conditions for the phase field problem we consider the sharp interface limit. To be precise, we show Γ-convergence of the reduced objective functional as the interfacial width, i.e., ε, tends to zero. Moreover, we show that the equations of the optimality systems converge. We hereby generalize findings from the literature where this result has already been indicated in [12] by formal asymptotics for certain objective functionals.

The paper is structured as follows: In section 2 we introduce the exact problem formulations and discuss well-posedness, optimality conditions, and the sharp interface limit. The derivation of the optimality conditions can be found in section 5, and some proofs of the sharp interface convergence results are collected in section 6. The numerical approach and results are given in section 3.

2. Discussion of the problems and convergence results.

2.1. Notation and assumptions. Before formulating the shape optimization problems we give a brief introduction of the most important quantities and equations in linearized elasticity and fix some notation. We refer the reader to [18, 19, 25] and references therein for details. We first assume to have in the hold-all container Ω two open subsets Ω_1 and Ω_2 which are separated by a hypersurface $\Gamma = \partial\Omega_1 \cap \partial\Omega_2$. The two subsets should correspond to two different elastic materials whose displacement fields are described by an unknown function $\boldsymbol{u} : \Omega \to \mathbb{R}^d$. To be precise, $\boldsymbol{u}|_{\Omega_i}$ corresponds to the displacement field of the ith material where $i \in \{1, 2\}$. We divide the boundary of Ω into two parts, one Dirichlet part where we can prescribe the displacement field and a Neumann part where the applied boundary forces are acting.

(A1) $\Omega \subset \mathbb{R}^d$ is a bounded Lipschitz domain with outer unit normal $\boldsymbol{n}$ and $d \in \{2, 3\}$. Moreover, assume $\partial\Omega = \Gamma_D \cup \Gamma_g$ with $\Gamma_D \cap \Gamma_g = \emptyset$ and $\mathcal{H}^{d-1}(\Gamma_D) > 0$, where $\mathcal{H}^{d-1}$ is the $(d-1)$-dimensional Hausdorff measure.

We remark that we denote $\mathbb{R}^d$-valued functions and spaces consisting of $\mathbb{R}^d$-valued functions in boldface.

For elastic materials the following equilibrium constraints hold in Ω_i, $i \in \{1, 2\}$:

$$-\nabla \cdot (\mathrm{D}_2 W_i (x, \mathcal{E}(\boldsymbol{u}))) = \boldsymbol{f} \qquad \text{in } \Omega_i, \tag{3a}$$

$$\mathrm{D}_2 W_i (x, \mathcal{E}(\boldsymbol{u})) \cdot \boldsymbol{n} = \boldsymbol{g} \qquad \text{on } \Gamma_g \cap \partial\Omega_i, \tag{3b}$$

$$\boldsymbol{u} = \boldsymbol{u}_D \qquad \text{on } \Gamma_D \cap \partial\Omega_i, \tag{3c}$$

where

(A2) $\boldsymbol{g} \in \boldsymbol{L}^2(\Gamma_g)$ is the given applied surface load, $\boldsymbol{f} \in \boldsymbol{L}^2(\Omega)$ is the given applied body force, and for simplicity we assume for the following considerations $\boldsymbol{u}_D \equiv \boldsymbol{0}$.

On the interface $\Gamma := \partial\Omega_1 \cap \partial\Omega_2$ we will assume standard transmission properties, i.e., the jump of $\mathrm{D}_2 W_i \cdot \boldsymbol{n}$ across the interface Γ is zero. In (5) we will see a weak formulation of these conditions. Moreover, $\mathcal{E}(\boldsymbol{u}) := \frac{1}{2}(\nabla \boldsymbol{u} + \nabla \boldsymbol{u}^T)$ is the so-called linearized strain, whereon the linear theory is based and $W_i : \Omega \times \mathbb{R}^{d \times d} \to \mathbb{R}$ denotes the elastic free energy density of the ith material. We use $W_i(x, \mathcal{E}) := \frac{1}{2}(\mathcal{E} - \overline{\mathcal{E}}_i) : \mathcal{C}_i(\mathcal{E} - \overline{\mathcal{E}}_i)$ for $\mathcal{E} \in \mathbb{R}^{d \times d}$, which is in our case independent of $x \in \mathbb{R}^d$. Here, $\mathcal{C}_i : \mathbb{R}^{d \times d} \to \mathbb{R}^{d \times d}$ is the elasticity tensor reflecting the material properties for material $i = 1$ and $i = 2$, respectively. Further, $\overline{\mathcal{E}}_i \in \mathbb{R}^{d \times d}$ is the eigenstrain which is given as the value of the strain when the ith material is unstressed. By $\mathrm{D}_2 W_i$ we denote the derivative with respect to the second component.

As already mentioned above, we have two different elastic materials inside the domain Ω. The design variable is a measurable function $\varphi : \Omega \to \mathbb{R}$, where $\{x \in \Omega \mid \varphi(x) = 1\} = \Omega_1$ describes the region where the first material is present up to a set of measure zero, and $\{x \in \Omega \mid \varphi(x) = -1\} = \Omega_2$ is the region which is filled with the second material. In the sharp interface setting, φ will only take values in $\{\pm 1\}$ and thus $\Omega = \Omega_1 \cup \Omega_2 \cup \Gamma$ with $\Gamma = \partial\Omega_1 \cap \partial\Omega_2$ being the separating hypersurface. In contrast, the phase field approximation uses a design function φ having values in $[-1, 1]$. Then, $\Omega = \Omega_1 \cup \Omega_2 \cup I$, where $I = \{-1 < \varphi < 1\}$ is the diffuse interface of small thickness approximating the hypersurface Γ. Using φ to describe the sharp as well as the diffuse interface model we describe the elasticity tensor and the eigenstrain as functions of the design variable φ which interpolate between two different values for the two different materials. We introduce the following assumptions on the elasticity tensor $\mathcal{C}$:

(A3) Let $\mathcal{C}(\varphi) = (\mathcal{C}_{ijkl}(\varphi))_{i,j,k,l=1}^d$ be such that $\mathcal{C}_{ijkl} \in C^{1,1}([-1,1])$ fulfills pointwise the following symmetry properties $\mathcal{C}_{ijkl}(\varphi) = \mathcal{C}_{jikl}(\varphi) = \mathcal{C}_{klij}(\varphi)$ for all $\varphi \in [-1,1]$, $i,j,k,l \in \{1,\ldots,d\}$. Moreover, we assume that there exist constants $C_C, c_C > 0$ such that

$$|\mathcal{C}(\varphi)A : B| \leq C_C\,|A|\,|B|\,, \quad \mathcal{C}(\varphi)A : A \geq c_C\,|A|^2 \tag{4}$$

holds for all symmetric matrices $A, B \in \mathbb{R}^{d\times d}$ and $\varphi \in [-1,1]$.

Remark 1.

1. The estimates (4) imply that the elasticity tensor interpolates between two finite positive definite tensors, and thus in particular no "void", i.e., regions without material, are allowed in this formulation.
2. The possibility of modeling void is given by using the so-called ersatz material approach, where a very soft material approximates the nonpresence of material; cf. [12, 17].
3. The elasticity tensor does not depend on the phase field parameter $\varepsilon > 0$ introduced later on. Hence, an ersatz material approach depending on the phase field parameter $\varepsilon > 0$ as it is employed in [12] cannot be used in this setting.

(A4) Let the eigenstrain $\overline{\mathcal{E}} \in C^{1,1}([-1,1], \mathbb{R}^{d\times d})$ be a function with symmetric values, i.e., $\overline{\mathcal{E}}(\varphi)^T = \overline{\mathcal{E}}(\varphi)$ for all $\varphi \in [-1,1]$.

Remark 2. Following Vegard's law, a commonly used assumption is that the eigenstrain interpolates linearly between the two values corresponding to the two materials. Then, assumption (A4) is fulfilled.

Using these assumptions, a weak formulation of the state equations on the whole of Ω can be derived if the design variable is $\varphi \in L^1(\Omega)$ with $|\varphi| \leq 1$ a.e. in Ω:

Find $\boldsymbol{u} \in \boldsymbol{H}^1_D(\Omega) := \{\boldsymbol{u} \in \boldsymbol{H}^1(\Omega) \mid \boldsymbol{u}|_{\Gamma_D} = \boldsymbol{0}\}$ such that

$$\int_\Omega \mathcal{C}\left(\varphi\right)\left(\mathcal{E}\left(\boldsymbol{u}\right) - \overline{\mathcal{E}}\left(\varphi\right)\right) : \mathcal{E}\left(\boldsymbol{v}\right)\,\mathrm{d}x = \int_\Omega \boldsymbol{f}\cdot\boldsymbol{v}\,\mathrm{d}x + \int_{\Gamma_g} \boldsymbol{g}\cdot\boldsymbol{v}\,\mathrm{d}s \quad \forall \boldsymbol{v} \in \boldsymbol{H}^1_D(\Omega). \tag{5}$$

In any subregion $\{\varphi = \pm 1\}$ this yields exactly the weak formulation of (3). The state equation is in both the phase field and the sharp interface formulation given by (5); cf. sections 2.2 and 2.3. Hence we directly state here the solvability result concerning this equation.

LEMMA 3. *For every $\varphi \in L^1(\Omega)$ with $|\varphi| \leq 1$ a.e. in Ω there exists a unique $\boldsymbol{u} \in \boldsymbol{H}^1_D(\Omega)$ such that (5) is fulfilled. Moreover, the solution $\boldsymbol{u}$ fulfills*

$$\|\boldsymbol{u}\|_{\boldsymbol{H}^1(\Omega)} \leq C\left(\Omega, \mathcal{C}, \overline{\mathcal{E}}\right)\Big(\|\boldsymbol{f}\|_{\boldsymbol{L}^2(\Omega)} + \|\boldsymbol{g}\|_{\boldsymbol{L}^2(\Gamma_g)} + 1\Big)\,. \tag{6}$$

This defines a solution operator $\boldsymbol{S} : \{\varphi \in L^1(\Omega) \mid |\varphi| \leq 1$ a.e. in $\Omega\} \to \boldsymbol{H}^1_D(\Omega)$.

Idea of the proof. By making use of Korn's inequality, this result is a direct consequence of the Lax–Milgram theorem; cf. [31, Lemma 24.1]. ∎

For our shape and topology optimization problem, the goal is to minimize

$$\mathbb{H}(\boldsymbol{u}) := \int_\Omega h_\Omega\left(x, \boldsymbol{u}\right)\,\mathrm{d}x + \int_{\Gamma_g} h_\Gamma\left(s, \boldsymbol{u}\right)\,\mathrm{d}s, \tag{7}$$

where h_Ω, h_Γ fulfill

(A5) $h_\Omega : \Omega \times \mathbb{R}^d \to \mathbb{R}$ and $h_\Gamma : \Gamma_g \times \mathbb{R}^d \to \mathbb{R}$ are Carathéodory functions, i.e.,
1. $h_\Omega(\cdot, \boldsymbol{v}) : \Omega \to \mathbb{R}$ and $h_\Gamma(\cdot, \boldsymbol{v}) : \Gamma_g \to \mathbb{R}$ are measurable for each $\boldsymbol{v} \in \mathbb{R}^d$, and
2. $h_\Omega(x, \cdot), h_\Gamma(s, \cdot) : \mathbb{R}^d \to \mathbb{R}$ are continuous for almost every $x \in \Omega$ and $s \in \Gamma_g$, respectively.

Moreover, assume that there exist functions $a_1 \in L^1(\Omega)$, $a_2 \in L^1(\Gamma_g)$ and $b_1 \in L^\infty(\Omega)$, $b_2 \in L^\infty(\Gamma_g)$ such that it holds that

$$|h_\Omega(x, \boldsymbol{v})| \le a_1(x) + b_1(x)|\boldsymbol{v}|^2 \quad \forall \boldsymbol{v} \in \mathbb{R}^d \text{ a.e. } x \in \Omega \tag{8}$$

and

$$|h_\Gamma(s, \boldsymbol{v})| \le a_2(s) + b_2(s)|\boldsymbol{v}|^2 \quad \forall \boldsymbol{v} \in \mathbb{R}^d \text{ a.e. } s \in \Gamma_g. \tag{9}$$

Additionally, we assume that the set

$$\left\{ \int_\Omega h_\Omega\left(x, \boldsymbol{S}(\varphi)(x)\right) \,\mathrm{d}x + \int_{\Gamma_g} h_\Gamma\left(s, \boldsymbol{S}(\varphi)(s)\right) \,\mathrm{d}s \mid \varphi \in L^1(\Omega), |\varphi| \le 1 \text{ a.e. in } \Omega \right\}$$

is bounded from below.

Remark 4. Due to [40], the Nemytskii operators

$$L^2(\Omega)^d \ni \boldsymbol{v} \mapsto h_\Omega\left(\cdot, \boldsymbol{v}\right) \in L^1(\Omega), \quad L^2(\Gamma_g)^d \ni \boldsymbol{v} \mapsto h_\Gamma\left(\cdot, \boldsymbol{v}\right) \in L^1(\Gamma_g)$$

are well-defined if and only if (8) and (9) are fulfilled and in this case the operators are continuous.

Assumptions (A1)–(A5) are the basic assumptions for the following considerations. To also derive first order optimality conditions we have to impose at some points additionally the following differentiability assumption.

(A6) For every fixed $\boldsymbol{v} \in \mathbb{R}^d$ we have $h_\Omega(\cdot, \boldsymbol{v}) \in W^{1,1}(\Omega)$ and $h_\Gamma(\cdot, \boldsymbol{v}) \in W^{1,1}(\Gamma_g)$. Let the partial derivatives $\mathrm{D}_2 h_\Omega(x, \cdot), \mathrm{D}_2 h_\Gamma(s, \cdot)$ exist for almost every $x \in \Omega$ and $s \in \Gamma_g$, respectively. Moreover there exist $\hat{a}_1 \in L^2(\Omega)$, $\hat{a}_2 \in L^2(\Gamma_g)$ and $\hat{b}_1 \in L^\infty(\Omega)$, $\hat{b}_2 \in L^\infty(\Gamma_g)$ such that

$$|\mathrm{D}_2 h_\Omega\left(x, \boldsymbol{v}\right)| \le \hat{a}_1(x) + \hat{b}_1(x)|\boldsymbol{v}| \quad \forall \boldsymbol{v} \in \mathbb{R}^d \text{ a.e. } x \in \Omega, \tag{10}$$

and

$$|\mathrm{D}_2 h_\Gamma\left(s, \boldsymbol{v}\right)| \le \hat{a}_2(s) + \hat{b}_2(s)|\boldsymbol{v}| \quad \forall \boldsymbol{v} \in \mathbb{R}^d \text{ a.e. } s \in \Gamma_g. \tag{11}$$

Remark 5. Under the assumption (A6) the operators

$$F : \boldsymbol{L}^2\left(\Omega\right) \ni \boldsymbol{u} \mapsto \int_\Omega h_\Omega\left(x, \boldsymbol{u}(x)\right) \,\mathrm{d}x, \quad G : \boldsymbol{L}^2(\Gamma_g) \ni \boldsymbol{u} \mapsto \int_{\Gamma_g} h_\Gamma\left(s, \boldsymbol{u}(s)\right) \,\mathrm{d}s$$

are continuously Fréchet differentiable and the directional derivatives are given by $\mathrm{D}F(\boldsymbol{u})(\boldsymbol{v}) = \int_\Omega \mathrm{D}_2 h_\Omega(x, \boldsymbol{u})\boldsymbol{v} \,\mathrm{d}x$, $\mathrm{D}G(\boldsymbol{u})(\boldsymbol{v}) = \int_{\Gamma_g} \mathrm{D}_2 h_\Gamma(s, \boldsymbol{u})\boldsymbol{v} \,\mathrm{d}s$.

In the next remark, we outline how we could replace assumptions (A5) and (A6) by weaker assumptions. In order to simplify the estimates in the following analysis we prefer (A5) and (A6).

Remark 6. We could generalize the results to objective functionals satisfying

$$|h_\Omega(x,\boldsymbol{v})| \leq a_1(x) + b_1(x)|\boldsymbol{v}|^p \quad \forall \boldsymbol{v} \in \mathbb{R}^d \text{ a.e. } x \in \Omega, \tag{12}$$

for some functions $a_1 \in L^1(\Omega)$ and $b_1 \in L^\infty(\Omega)$, instead of requiring (8). Here, $p \geq 2$ has to be chosen such that $\boldsymbol{H}^1(\Omega) \hookrightarrow \boldsymbol{L}^p(\Omega)$ is a compact embedding, and hence $2 \leq p < \infty$ for $d = 2$ and $2 \leq p < 6$ for $d = 3$. We then obtain that $L^p(\Omega)^d \ni \boldsymbol{v} \mapsto h_\Omega(\cdot,\boldsymbol{v}) \in L^1(\Omega)$ is well-defined and continuous and all proofs can be adapted. In this case, we have to replace (10) in assumption (A6) by $|\mathrm{D}_2 h_\Omega(x,\boldsymbol{v})| \leq \hat{a}_1(x) + \hat{b}_1(x)|\boldsymbol{v}|^{p-1}$ for all $\boldsymbol{v} \in \mathbb{R}^d$ and a.e. $x \in \Omega$, where $\hat{a}_1 \in L^{p/p-1}(\Omega)$, $\hat{b}_1 \in L^\infty(\Omega)$ to obtain that $\boldsymbol{L}^p(\Omega) \ni \boldsymbol{u} \mapsto \int_\Omega h_\Omega(x,\boldsymbol{u}(x))\,\mathrm{d}x$ is continuously Fréchet differentiable. The same holds for the choice of h_Γ.

In order to obtain a well-posed problem we add to the cost functional $\mathbb{H}$ in (7) a regularization term. In the sharp interface problem a multiple of the perimeter of the free boundary between the two materials is used. The exact definition of the perimeter is introduced now. Since we describe the sharp interface model by a design variable $\varphi : \Omega \to \{\pm 1\}$, where $\{\varphi = \pm 1\}$ describe the two different materials, this design variable is going to be a function of bounded variation. We give here a brief introduction in the notation of Caccioppoli sets and functions of bounded variations, but for a detailed introduction we refer to [6, 26]. We call a function $\varphi \in L^1(\Omega)$ a function of bounded variation if its distributional derivative is a vector-valued finite Radon measure. The space of functions of bounded variation in Ω is denoted by $BV(\Omega)$, and by $BV(\Omega,\{\pm 1\})$ we denote functions in $BV(\Omega)$ having only the values ± 1 a.e. in Ω; see [6] for details. We then call a measurable set $E \subset \Omega$ Caccioppoli set if $\chi_E \in BV(\Omega)$. For any Caccioppoli set E, one can hence define the total variation $|\mathrm{D}\chi_E|(\Omega)$ of $\mathrm{D}\chi_E$, as $\mathrm{D}\chi_E$ is a finite measure. This value is then called the perimeter of E in Ω and is denoted by $P_\Omega(E) := |\mathrm{D}\chi_E|(\Omega)$.

We include additionally a volume constraint in the optimization problem. By assuming that the design variable φ fulfills $\int_\Omega \varphi\,\mathrm{d}x \leq \beta|\Omega|$, which is equivalent to $|\{\varphi = 1\}| \leq \frac{(\beta+1)}{2}|\Omega|$ and $|\{\varphi = -1\}| \geq \frac{(1-\beta)}{2}|\Omega|$, for some fixed constant $\beta \in (-1,1)$ we prescribe a maximal amount of the material corresponding to $\{\varphi = 1\}$ (and thus a minimal amount of $\{\varphi = -1\}$) that can be used during the optimization process. Our admissible design variables for the sharp interface problem hence are chosen in the set

$$\Phi^0_{ad} := \left\{ \varphi \in BV(\Omega,\{\pm 1\}) \,\middle|\, \int_\Omega \varphi\,\mathrm{d}x \leq \beta|\Omega| \right\}. \tag{13}$$

In the phase field formulation of the shape optimization problem we approximate the perimeter by the Ginzburg–Landau energy

$$E_\varepsilon(\varphi) := \int_\Omega \frac{\varepsilon}{2}|\nabla\varphi|^2 + \frac{1}{\varepsilon}\psi(\varphi)\,\mathrm{d}x \tag{14}$$

with a double obstacle potential $\psi : \mathbb{R} \to \overline{\mathbb{R}} := \mathbb{R} \cup \{\infty\}$ given by

$$\psi(\varphi) := \begin{cases} \psi_0(\varphi) & \text{if } |\varphi| \leq 1, \\ +\infty & \text{if } |\varphi| > 1, \end{cases} \qquad \psi_0(\varphi) := \frac{1}{2}\left(1 - \varphi^2\right). \tag{15}$$

The functionals $(E_\varepsilon)_{\varepsilon>0}$ Γ-converge in $L^1(\Omega)$ to $\varphi \mapsto c_0 P_\Omega(\{\varphi = 1\})$ with $c_0 := \int_{-1}^1 \sqrt{2\psi(s)}\,\mathrm{d}s = \frac{\pi}{2}$ as $\varepsilon \searrow 0$; see, for instance, [16, 35, 36].

In the phase field setting, the design variable φ is allowed to have values in $[-1,1]$ and thus there may be a transition area between the areas $\{\varphi=-1\}$ and $\{\varphi=1\}$. The admissible set in the phase field setting is given by

$$\Phi_{ad} := \left\{ \varphi \in H^1(\Omega) \middle| \int_\Omega \varphi \, \mathrm{d}x \le \beta|\Omega|,\ |\varphi| \le 1 \text{ a.e. in } \Omega \right\} \tag{16}$$

and the extended admissible set by $\overline{\Phi}_{ad} := \{\varphi \in H^1(\Omega) \mid |\varphi| \le 1 \text{ a.e. in } \Omega\}$.

Remark 7. Instead of $\int_\Omega \varphi \, \mathrm{d}x \le \beta|\Omega|$ we could also use an equality constraint of the form $\int_\Omega \varphi \, \mathrm{d}x = \beta|\Omega|$. This prescribes then the exact volume fraction of each material in advance. In this setting, the same analysis can be carried out. Existing results in the literature, see, for instance [16, 27, 35], where we also base our sharp interface analysis on, only deal with equality constraints.

As we derive first order optimality conditions by varying the free boundary between the two materials with transformations, we introduce here the admissible transformations and its corresponding velocity fields.

DEFINITION 8 ($\mathcal{V}_{ad}$, $\mathcal{T}_{ad}$). *The space $\mathcal{V}_{ad}$ of admissible velocity fields is defined as the set of all $V \in C([-\tau,\tau] \times \overline{\Omega}, \mathbb{R}^d)$, where $\tau > 0$ is some fixed, small constant, such that it holds that*

- (V1) (V1a) $V(t,\cdot) \in C^2(\overline{\Omega}, \mathbb{R}^d)$,
  (V1b) $\exists C > 0$: $\|V(\cdot,y) - V(\cdot,x)\|_{C([-\tau,\tau],\mathbb{R}^d)} \le C|x-y|$ *for all* $x, y \in \overline{\Omega}$,
- (V2) $V(t,x) \cdot \boldsymbol{n}(x) = 0$ *for all* $x \in \partial\Omega$,
- (V3) $V(t,x) = \mathbf{0}$ *for every* $x \in \Gamma_D$.

Then the space $\mathcal{T}_{ad}$ of admissible transformations is defined as solutions of the ordinary differential equation

$$\partial_t T_t(x) = V(t, T_t(x)), \qquad T_0(x) = x \tag{17}$$

with $V \in \mathcal{V}_{ad}$, which gives some $T : (-\tilde{\tau}, \tilde{\tau}) \times \overline{\Omega} \to \overline{\Omega}$ with $0 < \tilde{\tau}$ small enough.

We often use the notation $V(t) = V(t,\cdot)$.

Remark 9. Let $V \in \mathcal{V}_{ad}$ and $T \in \mathcal{V}_{ad}$ be the transformation associated to V by (17). Then $T_t : \overline{\Omega} \to \overline{\Omega}$ is bijective and $T(\cdot,x) \in C^1((-\tau,\tau),\mathbb{R}^d)$ for all $x \in \overline{\Omega}$ and $\tau > 0$ small enough. These and other properties are discussed in detail in [21, 23].

We finish this introduction by two typical examples which are commonly used as objective functionals in structural optimization. For a deeper discussion on those problems and some further applications we refer, for instance, to [9].

Example 10 (mean compliance). One commonly used objective in structural optimization is the minimization of the mean compliance, which is for a structure in its equilibrium configuration given by $\int_\Omega \boldsymbol{f} \cdot \boldsymbol{u} \, \mathrm{d}x + \int_{\Gamma_g} \boldsymbol{g} \cdot \boldsymbol{u} \, \mathrm{d}s$. The aim of minimizing this objective functional can be interpreted as maximizing the stiffness under the given forces or as minimizing the stored mechanical energy. We notice that this is equivalent to minimizing $\int_\Omega \mathcal{C}(\varphi)(\mathcal{E}(\boldsymbol{u}) - \overline{\mathcal{E}}(\varphi)) : \mathcal{E}(\boldsymbol{u}) \, \mathrm{d}x$ if $\boldsymbol{u}$ solves the state equations (5).

Example 11 (compliant mechanism). The typical compliant mechanism objective functional used in topology optimization is given by the tracking type functional $\frac{1}{2}\int_\Omega c|\boldsymbol{u} - \boldsymbol{u}_\Omega|^2 \, \mathrm{d}x$, where $\boldsymbol{u}_\Omega \in \boldsymbol{L}^2(\Omega)$ is some desired displacement, and $c \in L^\infty(\Omega)$, $c \ge 0$, is a weighting factor.

In the following, by minimizers we always mean global minimizers.

2.2. Perimeter penalized shape optimization problem. The sharp interface problem that we consider in this section is given by

$$\min_{(\varphi,\boldsymbol{u})} J_0(\varphi,\boldsymbol{u}) := \mathbb{H}(\boldsymbol{u}) + \gamma c_0 P_\Omega(\{\varphi=1\}) = \int_\Omega h_\Omega(x,\boldsymbol{u})\,\mathrm{d}x + \int_{\Gamma_g} h_\Gamma(s,\boldsymbol{u})\,\mathrm{d}s + \gamma c_0 P_\Omega(\{\varphi=1\}) \tag{18}$$

with $(\varphi,\boldsymbol{u}) \in \Phi_{ad}^0 \times \boldsymbol{H}_D^1(\Omega)$ such that (5) holds, i.e.,

$$\int_\Omega \mathcal{C}(\varphi)\left(\mathcal{E}(\boldsymbol{u}) - \overline{\mathcal{E}}(\varphi)\right) : \mathcal{E}(\boldsymbol{v})\,\mathrm{d}x = \int_\Omega \boldsymbol{f}\cdot\boldsymbol{v}\,\mathrm{d}x + \int_{\Gamma_g} \boldsymbol{g}\cdot\boldsymbol{v}\,\mathrm{d}s \quad \forall \boldsymbol{v} \in \boldsymbol{H}_D^1(\Omega). \tag{19}$$

This is a topology and shape optimization problem, where $\varphi \in \Phi_{ad}^0 = \{\varphi \in BV(\Omega,\{\pm 1\}) \mid \int_\Omega \varphi\,\mathrm{d}x \le \beta|\Omega|\}$ plays the role of the design variable and can only have the discrete values ± 1. The perimeter in the cost functional ensures the existence of a minimizer where the weighting factor $\gamma > 0$ can be arbitrary. In the remainder of this subsection we summarize often results where the proofs are given later in this paper or in some previous work. Studying the reduced objective functional $j_0 : L^1(\Omega) \to \overline{\mathbb{R}}$,

$$j_0(\varphi) := \begin{cases} J_0(\varphi, \boldsymbol{S}(\varphi)) & \text{if } \varphi \in \Phi_{ad}^0, \\ +\infty & \text{otherwise,} \end{cases}$$

we obtain by using the direct method in the calculus of variations the well-posedness of the optimization problem.

THEOREM 12. *Under the assumptions* (A1)–(A5), *there exists at least one minimizer of* (18)–(19).

The proof is given in section 4.

Our next aim is to deduce first order necessary optimality conditions. For this purpose, we use the ideas of shape calculus, which means we apply geometric variations. As already mentioned in the introduction we do not impose any additional regularity assumption on the minimizing set. We obtain the following.

THEOREM 13. *Assume* (A1)–(A6). *Then for any minimizer* $(\varphi_0, \boldsymbol{u}_0) \in \Phi_{ad}^0 \times \boldsymbol{H}_D^1(\Omega)$ *of* (18)–(19) *the following necessary optimality conditions hold: There exists a Lagrange multiplier* $\lambda_0 \ge 0$ *for the integral constraint such that*

$$\partial_t|_{t=0} j_0\left(\varphi_0 \circ T_t^{-1}\right) = -\lambda_0 \int_\Omega \varphi_0 \operatorname{div} V(0)\,\mathrm{d}x, \quad \lambda_0\left(\int_\Omega \varphi_0\,\mathrm{d}x - \beta|\Omega|\right) = 0 \tag{20}$$

holds for all $T \in \mathcal{T}_{ad}$ *with corresponding velocity* $V \in \mathcal{V}_{ad}$, *where the derivative is given by the following formula:*

$$\partial_t|_{t=0} j_0\left(\varphi_0 \circ T_t^{-1}\right) = \partial_t|_{t=0} \mathbb{H}\left(\boldsymbol{S}\left(\varphi_0 \circ T_t^{-1}\right)\right) + \gamma c_0 \int_\Omega \left(\operatorname{div} V(0) - \nu \cdot \nabla V(0)\nu\right)\,\mathrm{d}\left|\mathrm{D}\chi_{E_0}\right| \tag{21}$$

and

$$\begin{aligned} &\partial_t|_{t=0} \mathbb{H}\left(\boldsymbol{S}\left(\varphi_0 \circ T_t^{-1}\right)\right) \\ &= \int_\Omega \left[\mathrm{D}h_\Omega(x,\boldsymbol{u}_0)\left(V(0), \dot{\boldsymbol{u}}_0[V]\right) + h_\Omega(x,\boldsymbol{u}_0)\operatorname{div} V(0)\right]\mathrm{d}x \\ &\quad + \int_{\Gamma_g} \left[\mathrm{D}h_\Gamma(s,\boldsymbol{u}_0)\left(V(0), \dot{\boldsymbol{u}}_0[V]\right) + h_\Gamma(s,\boldsymbol{u}_0)\left(\operatorname{div} V(0) - \boldsymbol{n}\cdot\nabla V(0)\boldsymbol{n}\right)\right]\mathrm{d}s \end{aligned} \tag{22}$$

with $\nu := \frac{\mathrm{D}\chi_{E_0}}{|\mathrm{D}\chi_{E_0}|}$ *being the generalized unit normal to* $E_0 := \{\varphi_0 = 1\}$ *defined on the reduced boundary of* E_0*; compare* [6]*. Moreover,* $\dot{\boldsymbol{u}}_0[V] \in \boldsymbol{H}^1_D(\Omega)$ *is given as the solution of*

$$
\begin{aligned}
&\int_\Omega \mathcal{C}(\varphi_0)\mathcal{E}(\dot{\boldsymbol{u}}_0[V]) : \mathcal{E}(\boldsymbol{v})\,\mathrm{d}x \\
&\quad= \int_\Omega \mathcal{C}(\varphi_0)\frac{1}{2}\left(\nabla V(0)\nabla \boldsymbol{u}_0 + (\nabla V(0)\nabla \boldsymbol{u}_0)^T\right) : \mathcal{E}(\boldsymbol{v}) \\
&\qquad+ \mathcal{C}(\varphi_0)\left(\mathcal{E}(\boldsymbol{u}_0) - \overline{\mathcal{E}}(\varphi_0)\right) : \frac{1}{2}\left(\nabla V(0)\nabla \boldsymbol{v} + (\nabla V(0)\nabla \boldsymbol{v})^T\right) \\
&\qquad- \mathcal{C}(\varphi_0)\left(\mathcal{E}(\boldsymbol{u}_0) - \overline{\mathcal{E}}(\varphi_0)\right) : \mathcal{E}(\boldsymbol{v})\,\mathrm{div}\,V(0)\,\mathrm{d}x \\
&\qquad- \int_\Omega \boldsymbol{f}\cdot \mathrm{D}\boldsymbol{v}V(0)\,\mathrm{d}x - \int_{\Gamma_g} \boldsymbol{g}\cdot \mathrm{D}\boldsymbol{v}V(0)\,\mathrm{d}s,
\end{aligned} \tag{23}
$$

which has to hold for all $\boldsymbol{v} \in \boldsymbol{H}^1_D(\Omega)$*.*

The proof of this theorem can be found in section 5.

Remark 14. If we assume that Γ_g has C^2-regularity, (22) can be rewritten into a more convenient form by using the identity $\mathrm{div}_{\Gamma_g} V(0) = \mathrm{div}\,V(0) - \boldsymbol{n}\cdot\nabla V(0)\boldsymbol{n}$ on Γ_g.

We can now reformulate those optimality conditions under more regularity assumptions on the minimizing set $E_0 = \{\varphi_0 = 1\}$ and the given data. In particular, we can then compare our results to those obtained in literature; see Remark 16.

THEOREM 15. *Assume* (A1)–(A6)*. Let* $(\varphi_0, \boldsymbol{u}_0) \in \Phi^0_E \times \boldsymbol{H}^1_D(\Omega)$ *be minimizers of* (18)–(19)*. Assume there are open sets* $\Omega_1, \Omega_2 \subset \Omega$ *such that* $\varphi_0 = 1$ *a.e. on* Ω_1 *and* $\varphi_0 = -1$ *a.e. in* Ω_2*. Let* $\boldsymbol{g} \in \boldsymbol{H}^{\frac{1}{2}}(\partial\Omega)$ *and the objective functional is assumed to be chosen in such a way that* $\mathrm{D}_2 h_\Omega(\cdot, \boldsymbol{u}) \in \boldsymbol{L}^2(\Omega)$ *and* $\mathrm{D}_2 h_\Gamma(\cdot, \boldsymbol{u}) \in \boldsymbol{H}^{\frac{1}{2}}(\Gamma_g)$ *for all* $\boldsymbol{u} \in \boldsymbol{H}^1(\Omega)$*. If* $h_\Gamma(\cdot, \boldsymbol{u}_0(\cdot)) \not\equiv 0$*, we assume additionally that* Γ_g *has* C^2*-regularity. Assume that* $\Gamma_0 := \partial\Omega_1 \cap \partial\Omega_2 \in C^2$ *and* $d(\Gamma_0, \partial\Omega) > 0$*. By* $[\boldsymbol{w}]_{\Gamma_0}(x) := \boldsymbol{w}|_{\Omega_1}(x) - \boldsymbol{w}|_{\Omega_2}(x)$ *we denote the jump of* $\boldsymbol{w}$ *along the interface* Γ_0*, and* ν *is the outer unit normal on* Ω_1*. Let* $\kappa = \mathrm{div}_{\Gamma_0}\nu$ *be the mean curvature of* Γ_0*. Then the optimality conditions derived in Theorem* 13 *are equivalent to the following system:*

$$
\left.
\begin{aligned}
\gamma c_0 \kappa - &\left[\mathcal{C}(\varphi_0)\left(\mathcal{E}(\boldsymbol{u}_0) - \overline{\mathcal{E}}(\varphi_0)\right) : \mathcal{E}(\boldsymbol{q}_0)\right]_{\Gamma_0} \\
&+ \left[\mathcal{C}(\varphi_0)\left(\mathcal{E}(\boldsymbol{u}_0) - \overline{\mathcal{E}}(\varphi_0)\right)\nu \cdot \partial_\nu \boldsymbol{q}_0\right]_{\Gamma_0} \\
&+ \left[\mathcal{C}(\varphi_0)\mathcal{E}(\boldsymbol{q}_0)\,\nu\cdot\partial_\nu \boldsymbol{u}_0\right]_{\Gamma_0} + 2\lambda_0 + \left[h_\Omega(x, \boldsymbol{u}_0)\right]_{\Gamma_0} = 0 \quad \text{on } \Gamma_0
\end{aligned}
\right\} \tag{24}
$$

$$
\lambda_0\left(\int_\Omega \varphi_0\,\mathrm{d}x - \beta|\Omega|\right) = 0,\ \lambda_0 \geq 0,\ \int_\Omega \varphi_0\,\mathrm{d}x \leq \beta|\Omega|, \tag{25}
$$

together with the state equation (5) *relating* φ_0 *and* $\boldsymbol{u}_0$*. Here, the adjoint variable* $\boldsymbol{q}_0 \in \boldsymbol{H}^1_D(\Omega)$ *is the unique solution of the adjoint equation*

$$
\begin{aligned}
\int_\Omega \mathcal{C}(\varphi_0)\mathcal{E}(\boldsymbol{q}_0) : \mathcal{E}(\boldsymbol{v})\,\mathrm{d}x &= \int_\Omega \mathrm{D}_2 h_\Omega(x, \boldsymbol{u}_0)\,\boldsymbol{v}\,\mathrm{d}x \\
&\quad+ \int_{\Gamma_g} \mathrm{D}_2 h_\Gamma(s, \boldsymbol{u}_0)\,\boldsymbol{v}\,\mathrm{d}s \quad \forall \boldsymbol{v} \in \boldsymbol{H}^1_D(\Omega).
\end{aligned} \tag{26}
$$

We refer to section 5 for a sketch of the main steps in the proof of the previous theorem.

Remark 16. In [12] the same optimality system for the sharp interface setting has been derived from the phase field model by formally matched asymptotics for the mean compliance and compliant mechanism problems mentioned in Examples 10 and 11. However, no eigenstrain has been taken into account in [12], while this is included in the above problem setting. Applying shape sensitivity analysis yields the same result as we have found in Theorem 15 (see, e.g., [1, 4, 42] and [11, 32, 33, 37] for related problems).

2.3. Phase field approximation. In a diffuse interface setting in terms of a phase field formulation the shape and topology optimization problem of finding the optimal material distribution of two given materials is given by

$$\begin{aligned}\min_{(\varphi,\boldsymbol{u})} J_\varepsilon(\varphi,\boldsymbol{u}) &:= \mathbb{H}(\boldsymbol{u}) + \gamma E_\varepsilon(\varphi) \\ &= \int_\Omega h_\Omega(x,\boldsymbol{u})\,\mathrm{d}x + \int_{\Gamma_g} h_\Gamma(s,\boldsymbol{u})\,\mathrm{d}s + \gamma\int_\Omega \frac{\varepsilon}{2}|\nabla\varphi|^2 + \frac{1}{\varepsilon}\psi(\varphi)\,\mathrm{d}x \end{aligned} \tag{27}$$

with $(\varphi,\boldsymbol{u}) \in \Phi_{ad} \times \boldsymbol{H}^1_D(\Omega)$ such that (5) holds, i.e.,

$$\int_\Omega \mathcal{C}(\varphi)\left(\mathcal{E}(\boldsymbol{u}) - \overline{\mathcal{E}}(\varphi)\right) : \mathcal{E}(\boldsymbol{v})\,\mathrm{d}x = \int_\Omega \boldsymbol{f}\cdot\boldsymbol{v}\,\mathrm{d}x + \int_{\Gamma_g} \boldsymbol{g}\cdot\boldsymbol{v}\,\mathrm{d}s \quad \forall \boldsymbol{v} \in \boldsymbol{H}^1_D(\Omega). \tag{28}$$

Hence the design variable in this problem is given by $\varphi \in \Phi_{ad} = \{\varphi \in H^1(\Omega) \mid \int_\Omega \varphi\,\mathrm{d}x \le \beta|\Omega|,\ |\varphi| \le 1 \text{ a.e. in } \Omega\}$. The regions filled with material one or two are represented by $\{x \in \Omega \mid \varphi(x) = 1\}$ and $\{x \in \Omega \mid \varphi(x) = -1\}$, respectively. The design variable φ is also allowed to take values between minus one and one, which leads to a small transitional area whose thickness is proportional to a small parameter $\varepsilon > 0$. Thus, as ε tends to zero, we will arrive in a sharp interface problem and the interfacial layer vanishes.

As was already discussed in section 2.1, the Ginzburg–Landau energy E_ε, compare (14), appearing in the objective functional is essential for the existence of a minimizer and $(E_\varepsilon)_\varepsilon$ Γ-converge to a multiple of the perimeter functional as ε tends to zero; cf. [35, 36]. The parameter $\gamma > 0$ is an arbitrary fixed constant and can be considered as a weighting factor of the perimeter penalization.

We know from Lemma 3 that there is a solution operator $\boldsymbol{S}$ for the constraints (28). Thus, we can reformulate the optimization problem into $\min_{\varphi\in L^1(\Omega)} j_\varepsilon(\varphi)$, where $j_\varepsilon : L^1(\Omega) \to \overline{\mathbb{R}}$,

$$j_\varepsilon(\varphi) := \begin{cases} J_\varepsilon(\varphi, \boldsymbol{S}(\varphi)) & \text{if } \varphi \in \Phi_{ad}, \\ +\infty & \text{otherwise,} \end{cases}$$

is the reduced objective functional. We start by discussing the optimization problem (27)–(28) in view of well-posedness for fixed $\varepsilon > 0$.

THEOREM 17. *Under the assumptions* (A1)–(A5), *there exists at least one minimizer of* (27)–(28).

A sketch of the proof will be given in section 4.

We obtain optimality conditions by geometric variations.

THEOREM 18. *Assume* (A1)–(A6). *Then for any minimizer* $(\varphi_\varepsilon, \boldsymbol{u}_\varepsilon)$ *of* (27)–(28) *the following necessary optimality conditions hold: There exists a Lagrange multiplier* $\lambda_\varepsilon \ge 0$ *for the integral constraint such that*

$$\partial_t|_{t=0} j_\varepsilon\left(\varphi_\varepsilon \circ T_t^{-1}\right) = -\lambda_\varepsilon \int_\Omega \varphi_\varepsilon \operatorname{div} V(0)\,\mathrm{d}x, \quad \lambda_\varepsilon\left(\int_\Omega \varphi_\varepsilon\,\mathrm{d}x - \beta|\Omega|\right) = 0 \tag{29}$$

holds for all $T \in \mathcal{T}_{ad}$ *with corresponding velocity* $V \in \mathcal{V}_{ad}$. *The derivative is given by* *the following formula:*

$$\begin{aligned}(30)\quad &\partial_t|_{t=0} j_\varepsilon\left(\varphi_\varepsilon \circ T_t^{-1}\right) = \partial_t|_{t=0} \mathbb{H}\left(\boldsymbol{S}\left(\varphi_\varepsilon \circ T_t^{-1}\right)\right) \\ &\quad + \int_\Omega \Big(\frac{\gamma\varepsilon}{2}\left|\nabla\varphi_\varepsilon\right|^2 + \frac{\gamma}{\varepsilon}\psi\left(\varphi_\varepsilon\right)\Big) \operatorname{div} V(0) - \gamma\varepsilon\nabla\varphi_\varepsilon \cdot \nabla V(0) \nabla\varphi_\varepsilon \,\mathrm{d}x,\end{aligned}$$

where $\dot{\boldsymbol{u}}_\varepsilon[V] \in \boldsymbol{H}^1_D(\Omega)$ *is given as the solution of* (23) *with* φ_0 *replaced by* φ_ε *and* $\boldsymbol{u}_0$ *by* $\boldsymbol{u}_\varepsilon$. *The exact formula for* $\partial_t|_{t=0}\mathbb{H}(\boldsymbol{S}(\varphi_\varepsilon \circ T_t^{-1}))$ *is given in* (22).

The proof can be found in section 5.

Remark 19. One can also consider (27)–(28) in the framework of optimal control problems. By parametric variations one then obtains as necessary optimality conditions the following variational inequality:

$$(31)\qquad j_\varepsilon'(\varphi_\varepsilon)(\varphi - \varphi_\varepsilon) + \lambda_\varepsilon \int_\Omega (\varphi - \varphi_\varepsilon)\,\mathrm{d}x \geq 0 \quad \forall \varphi \in \overline{\Phi}_{ad},$$

where

$$\begin{aligned}(32)\quad & j_\varepsilon'(\varphi_\varepsilon)(\varphi - \varphi_\varepsilon) \\ &= \left(\gamma\varepsilon\nabla\varphi_\varepsilon, \nabla\left(\varphi - \varphi_\varepsilon\right)\right)_{\boldsymbol{L}^2(\Omega)} \\ &\quad + \Big(\frac{\gamma}{\varepsilon}\psi_0'\left(\varphi_\varepsilon\right) + \Big(\mathcal{C}(\varphi_\varepsilon)\overline{\mathcal{E}}'\left(\varphi_\varepsilon\right) - \mathcal{C}'\left(\varphi_\varepsilon\right)\left(\mathcal{E}\left(\boldsymbol{u}_\varepsilon\right) - \overline{\mathcal{E}}\left(\varphi_\varepsilon\right)\right)\Big) : \mathcal{E}\left(\boldsymbol{q}_\varepsilon\right), \varphi - \varphi_\varepsilon\Big)_{L^2(\Omega)}\end{aligned}$$

is the directional derivative of the reduced objective functional j_ε. The variational inequality (31) has to be fulfilled together with the state equations (28) and the adjoint equation (26). This approach can, for instance, be used for numerical methods. More details on these optimality criteria can be found in [12, 31].

2.4. Sharp interface limit. In this section we give the results on relating the phase field problems introduced in section 2.3 to the sharp interface formulation, which was discussed in Section 2.2.

THEOREM 20. *Under the assumptions* (A1)–(A5), *the functionals* $(j_\varepsilon)_{\varepsilon>0}$ Γ*-converge in* $L^1(\Omega)$ *to* j_0 *as* $\varepsilon \searrow 0$.

We also refer to Penzler, Rumpf, and Wirth [38], who studied a related Γ-limit under different assumptions and in the context of nonlinear elasticity. The proof of this theorem is given in section 6. As a consequence, we obtain directly the following.

COROLLARY 21. *Assume* (A1)–(A5). *Let* $(\varphi_\varepsilon)_{\varepsilon>0}$ *be minimizers of* $(j_\varepsilon)_{\varepsilon>0}$. *Then there exists a subsequence, denoted by the same, and an element* $\varphi_0 \in L^1(\Omega)$ *such that* $\lim_{\varepsilon\searrow 0}\|\varphi_\varepsilon - \varphi_0\|_{L^1(\Omega)} = 0$. *Besides,* φ_0 *is a minimizer of* j_0 *and it holds that* $\lim_{\varepsilon\searrow 0} j_\varepsilon(\varphi_\varepsilon) = j_0(\varphi_0)$.

Proof. From $\sup_{\varepsilon>0} j_\varepsilon(\varphi_\varepsilon) < \infty$ we find $\sup_{\varepsilon>0}\int_\Omega(\frac{\varepsilon}{2}|\nabla\varphi_\varepsilon|^2 + \frac{1}{\varepsilon}\psi(\varphi_\varepsilon))\,\mathrm{d}x < \infty$. Using compactness arguments [35, Proposition 3] one can show that the functionals $\varphi_\varepsilon \to \int_\Omega \frac{\varepsilon}{2}|\nabla\varphi_\varepsilon|^2 + \frac{1}{\varepsilon}\psi(\varphi_\varepsilon)\,\mathrm{d}x$ are equicoercive in $L^1(\Omega)$, and one hence finds a subsequence of $(\varphi_\varepsilon)_{\varepsilon>0}$ converging in $L^1(\Omega)$ to some element φ_0 as $\varepsilon \searrow 0$, see [20]. Then the previous theorem and standard results for Γ-convergence, see, for instance, [20], yield the assertion. ∎

THEOREM 22. *Assume* (A1)–(A6). *Let* $(\varphi_\varepsilon)_{\varepsilon>0}$ *be minimizers of* $(j_\varepsilon)_{\varepsilon>0}$. *Then there exists a subsequence, which is denoted by the same, that converges in* $L^1(\Omega)$ *to a* *minimizer* φ_0 *of* j_0. *Moreover, it holds that* $\lim_{\varepsilon\searrow 0}\partial_t|_{t=0} j_\varepsilon(\varphi_\varepsilon\circ T_t^{-1}) = \partial_t|_{t=0} j_0(\varphi_0\circ T_t^{-1})$ *for all* $T\in\mathcal{T}_{ad}$. *If* $|\{\varphi_0 = 1\}| > 0$, *then we additionally have the following convergence results:*

$$\boldsymbol{u}_\varepsilon \overset{\varepsilon\searrow 0}{\rightharpoonup} \boldsymbol{u}_0, \quad \dot{\boldsymbol{u}}_\varepsilon[V] \overset{\varepsilon\searrow 0}{\rightharpoonup} \dot{\boldsymbol{u}}_0[V] \qquad \text{in } \boldsymbol{H}^1(\Omega), \tag{33a}$$

$$\lambda_\varepsilon \overset{\varepsilon\searrow 0}{\longrightarrow} \lambda_0, \quad j_\varepsilon(\varphi_\varepsilon) \overset{\varepsilon\searrow 0}{\longrightarrow} j_0(\varphi_0) \qquad \text{in } \mathbb{R}, \tag{33b}$$

where $\boldsymbol{u}_\varepsilon = \boldsymbol{S}(\varphi_\varepsilon)$, $\boldsymbol{u}_0 = \boldsymbol{S}(\varphi_0)$, *and* $(\lambda_\varepsilon)_{\varepsilon>0}\subseteq\mathbb{R}_0^+$ *are Lagrange multipliers for the integral constraint defined in Theorem* 18, *and* $\lambda_0\in\mathbb{R}_0^+$ *is a Lagrange multiplier for the integral constraint in the sharp interface setting since it fulfills* (20).

The proof is given in section 6.

3. Numerical experiments. We want to verify the reliability and practical relevance of the phase field approximation by means of numerical experiments. Besides, we also study the behavior for decreasing phase field parameters $\varepsilon > 0$ and see that the convergence results stated in the previous section are also indicated by numerics. For the numerics, the admissible design functions are chosen in $\widetilde{\Phi}_{ad} := \{\varphi\in H^1(\Omega) \mid \int_\Omega \varphi\,\mathrm{d}x = \beta|\Omega|,\ |\varphi|\le 1 \text{ a.e. in } \Omega\}$ instead of $\varphi\in\Phi_{ad}$. Thus, the integral volume constraint is replaced by an equality constraint, which means that we prescribe the exact volume fraction in advance. As already discussed in Remark 7, this does not change the analytical results presented in the previous section. The only difference is that the Lagrange multipliers $\lambda_\varepsilon\in\mathbb{R}$ are also allowed to be negative and the complementarity conditions are fulfilled trivially.

3.1. Description of algorithm. On the reduced problem formulation we apply an extension of the projected gradient method $\varphi_{k+1} = \varphi_k + \alpha_k\mathcal{P}(\varphi_k - \nabla j_\varepsilon(\varphi_k))$, where $\mathcal{P}$ denotes the projection on the admissable set $\widetilde{\Phi}_{ad}$, without requiring the existence of a gradient. In addition, we allow for a variable scalar scaling $\zeta_k > 0$ of the derivative, as well as the use of a variable inner product for the projection and the gradient, which can include second order information. The step length is determined by Armijo backtracking. For more details, see [13, 15].

ALGORITHM 1.

Choose $0<\beta<1$, $0<\sigma<1$ *and* $\varphi_0\in\widetilde{\Phi}_{ad}$; *set* $k := 0$.
while $k\le k_{max}$ ***do***
  Choose $\zeta_k > 0$ *and an inner product* a_k.
  Calculate the minimum $\overline{\varphi}_k = \mathcal{P}_k(\varphi_k)$ *of the projection-type subproblem*

$$\min_{y\in\widetilde{\Phi}_{ad}} \quad \frac{1}{2}\|y-\varphi_k\|_{a_k}^2 + \zeta_k j_\varepsilon'(\varphi_k)(y-\varphi_k). \tag{34}$$

  Set the search direction $v_k := \overline{\varphi}_k - \varphi_k$
  if $\sqrt{\varepsilon\gamma}\|\nabla v_k\|_{L^2} < tol$, ***then***
    return
  end if
  Determine the step length $\alpha_k := \beta^{m_k}$ *with minimal* $m_k\in\mathbb{N}_0$ *such that* $j_\varepsilon(\varphi_k+\alpha_k v_k)\le j_\varepsilon(\varphi_k) + \alpha_k\sigma\langle j_\varepsilon'(\varphi_k), v_k\rangle$.
  Update $\varphi_{k+1} := \varphi_k + \alpha_k v_k$,
  $k := k+1$,
end while

The maximal number of iterations $k_{\max}$ is set to 10^5 in the experiments below. The directional derivative $j'_\varepsilon(\varphi_k)v$ is given in (32). We start with small ζ_k to enhance the convergence of the primal dual active set (PDAS) method and increase it slowly in every step until $\zeta_k = 1$. The inner product a_k is initialized choosing $a_0(\xi,\eta) = \varepsilon\gamma\int_\Omega \nabla\xi \cdot \nabla\eta \,\mathrm{d}x$. To get faster convergence, we update the inner product a_k in every step by a BFGS update whenever possible; see [15] for details. Note that the solution $\overline{\varphi}_k$ to the projection-type subproblem (34) is formally given by $\overline{\varphi}_k = P_{a_k}(\varphi_k - \zeta_k \nabla_{a_k} j_\varepsilon(\varphi_k))$, where P_{a_k} denotes the orthogonal projection onto $\widetilde{\Phi}_{ad}$ with respect to the inner product a_k and $\nabla_{a_k} j_\varepsilon(\varphi_k)$ denotes the Riesz representative of $j'_\varepsilon(\varphi_k)$ with respect to the inner product a_k. This is only formally since j_ε need not be differentiable with respect to the norm induced by a_k. The subproblem (34) is solved by a PDAS method; see [10, 14].

Remark 23. In [15] it is shown that every accumulation point of the sequence $(\varphi_k)_{k\in\mathbb{N}}$ in the $H^1(\Omega) \cap L^\infty(\Omega)$ topology is a stationary point of j_ε and that $\lim_{k\to\infty} \|v_k\|_{H^1(\Omega)} = 0$. Additionally mesh independence can be observed.

For all of our numerical experiments we consider the compliance problem, see Example 10, and assume to have only the external surface load $\boldsymbol{g}$, and hence $\boldsymbol{f} \equiv \mathbf{0}$. Thus we choose $h_\Omega(x,\boldsymbol{u}) = 0$, $h_\Gamma(x,\boldsymbol{u}) = \boldsymbol{g}\cdot\boldsymbol{u}$. In the following examples $\boldsymbol{g}$ will always be an element in $\boldsymbol{L}^\infty(\Gamma_g)$ and so assumption (A5) is fulfilled. Thus the objective functional is given in the following numerical experiments by

$$j_\varepsilon(\varphi) = \int_{\Gamma_g} \boldsymbol{g}\cdot\boldsymbol{S}(\varphi)\,\mathrm{d}s + \gamma\int_\Omega \frac{\varepsilon}{2}|\nabla\varphi|^2 + \frac{1}{2\varepsilon}\left(1-\varphi^2\right)\,\mathrm{d}x.$$

The used elasticity tensor interpolates between its two values quadratically. Inside the first material (represented by $\varphi = 1$) and the second material (represented by $\varphi = -1$) it is given by the two Lamé constants λ_1, μ_1 and λ_2, μ_2, respectively. We choose $\mathcal{C}(\varphi)\mathcal{E} := 2\iota_{\delta_\mu}(\varphi)\mu_2\mathcal{E} + \iota_{\delta_\lambda}(\varphi)\lambda_2\mathrm{tr}(\mathcal{E})I$, where $\iota_\delta(\varphi) = 0.25(1-\delta)\varphi^2 - 0.5(1-\delta)\varphi + 0.25(1-\delta) + \delta$, and thus $\iota_\delta(1) = 1$ and $\iota_\delta(-1) = \delta$, and $\delta_\mu := \mu_1/\mu_2$, $\delta_\lambda := \lambda_1/\lambda_2$.

The phase field φ and the state equation are discretized using standard piecewise linear finite elements. An adaptive mesh is implemented, which is fine on the interface and coarse in the bulk region as described in [7]. All appearing integrals are computed by exact quadrature rules.

3.2. Optimal design of a cantilever beam. The first experiment is carried out in the design domain $\Omega = (-1,1)\times(0,1)$, and we choose $\Gamma_D := \{(x,y)\in\partial\Omega \mid x = -1\}$ and the support of the force $\boldsymbol{g}$ will be concentrated on $\Gamma_g^0 := \{(x,y)\in\partial\Omega \mid x \geq 0.75, y = 0\} \subset \Gamma_g$. The surface load is chosen to be $\boldsymbol{g} = (0,-250)^T\chi_{\Gamma_g^0}$, and there is no eigenstrain, i.e., $\overline{\mathcal{E}} = 0$. The configuration is sketched in Figure 1(a), and the initial shape always corresponds to $\varphi \equiv 0$. Thus, also $\beta = 0$ is chosen for the volume constraint. The first material, represented by $\varphi = 1$ is given by the constants $\lambda_1 = \mu_1 = 5000$ and the second material (i.e., $\varphi = -1$) is a more elastic material with $\lambda_2 = \mu_2 = 10$. Lamé constants with such a pronounced contrast also appear in applications; compare [39]. A uniform mesh size of $h = 2^{-6}$ is chosen on the bulk and the interfacial layer is refined such that there are eight mesh points across the interface. Since the interface thickness is proportional to ε, the mesh has to be chosen finer on the interface as ε gets smaller.

Results for minimizing the mean compliance of a cantilever beam for three different phase field parameters ε are shown in Figure 2. Here we chose the weighting factor for the Ginzburg–Landau energy $\gamma = 0.5$. Already for $\varepsilon = 0.06$ one obtains the

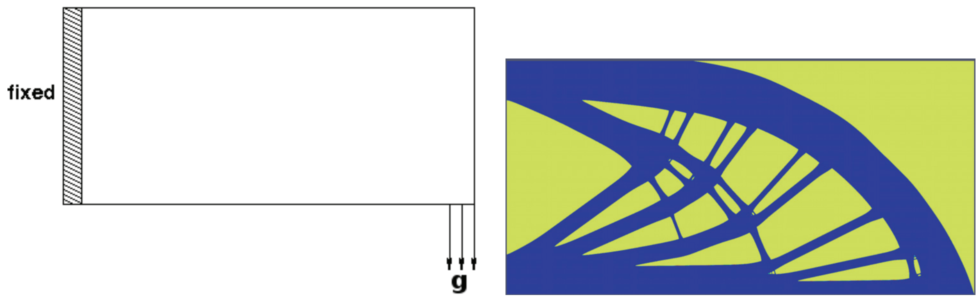

(a) Configuration of the cantilever beam.

(b) Optimal configuration for $\gamma = 0.002$. The stiff material is blue.

FIG. 1. *Cantilever beam.*

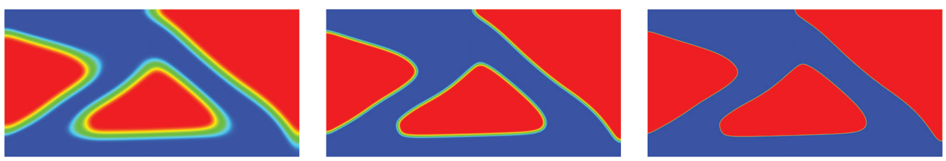

(a) $\varepsilon = 0.06$

(b) $\varepsilon = 0.015$

(c) $\varepsilon = 0.001875$

FIG. 2. *Optimal material configuration φ_ε for the cantilever beam for $\gamma = 0.5$ and different values of ε (stiff material in blue, weak material in red, and interface in green).*

same structure as for the smallest value of the phase field parameter, i.e., the right qualitative behavior of the sharp interface minimizer. We also remark that for the smallest value of ε, the interface is already very thin and almost not visible anymore.

We want to study the convergence of the minimizers $(\varphi_\varepsilon)_\varepsilon$. For this purpose we denote by φ_0 a minimizer for the sharp interface problem. As this minimizer is a priori unknown, we approximate φ_0 by $\tilde{\varphi}_0 := 2\chi_{\{\varphi_{\varepsilon_{\min}}>0\}} - 1$, where $\varepsilon_{\min} := 0.001875$. Thus the optimal interface Γ_0 is approximated by the zero level set of $\varphi_{\varepsilon_{\min}}$, denoted by $\tilde{\Gamma}_0$. The difference $\|\varphi_\varepsilon - \tilde{\varphi}_0\|_{L^1(\Omega)}$ can be separated into two terms,

$$\|\varphi_\varepsilon - \tilde{\varphi}_0\|_{L^1(\Omega)} \sim \|\varphi_\varepsilon - \varphi_\varepsilon^o\|_{L^1(\Omega)} + \|\varphi_\varepsilon^o - \tilde{\varphi}_0\|_{L^1(\Omega)} \tag{35}$$

where $(\varphi_\varepsilon^o)_\varepsilon$ denotes the constructed recovery sequence corresponding to $\tilde{\varphi}_0$ and exposes a sin-profile normal to $\tilde{\Gamma}_0$; see [16]. We want to determine which term of the error in (35) is the dominating part. We notice that the first term on the right-hand side of (35) can be considered as the distance of the zero level sets of φ_ε and $\varphi_{\varepsilon_{\min}}$ and the second term describes the error resulting from the diffuse interface profile. The one-dimensional error of the sin-profile compared to a characteristic function is given by $\int_{-\varepsilon\pi/2}^{\varepsilon\pi/2} |\sin(\frac{x}{\varepsilon}) - \operatorname{sgn}(x)|\,\mathrm{d}x = (\pi-2)\varepsilon$. Thus, the $L^1(\Omega)$-error in our two-dimensional setting can be approximated by $\|\varphi_\varepsilon^o - \tilde{\varphi}_0\|_{L^1(\Omega)} \approx P_\Omega(\{\varphi_0 = 1\})(\pi-2)\varepsilon$. As the perimeter $P_\Omega(\{\varphi_0 = 1\})$ is not known, we extrapolate the given sequence $(E_\varepsilon(\varphi_\varepsilon))_\varepsilon$ numerically to $\varepsilon = 0$, which gives $\lim_{\varepsilon\searrow 0} E_\varepsilon(\varphi_\varepsilon) \approx e_0 := 8.1754$. As mentioned above, from the Γ-convergence result of [16, 35] it is expected that $e_0 \approx \frac{\pi}{2} P_\Omega(\{\varphi_0 = 1\})$. Hence, we may approximate $\|\varphi_\varepsilon^o - \tilde{\varphi}_0\|_{L^1(\Omega)} \approx m\varepsilon$ with $m := \frac{2(\pi-2)}{\pi} e_0$.

In Figure 3(a) we now depict the difference $\|\varphi_\varepsilon - \tilde{\varphi}_0\|_{L^1(\Omega)}$ (solid blue line) together with the approximated diffuse interface error $m\varepsilon$ (dashed red line). We see that for $\varepsilon < 0.02$ the L^1-difference of the minimizer φ_ε and the approximated minimizer $\tilde{\varphi}_0$

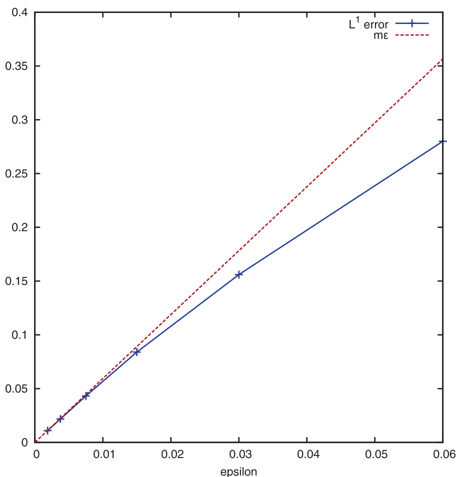

(a) The solid blue line shows $\|\varphi_\varepsilon - \tilde{\varphi}_0\|_{L^1(\Omega)}$. The approximated diffuse interface error is depicted in the red, dashed line.

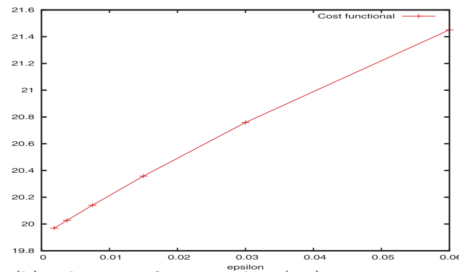

(b) The cost functional $j_\varepsilon(\varphi_\varepsilon)$ seems to converge as $\varepsilon \searrow 0$.

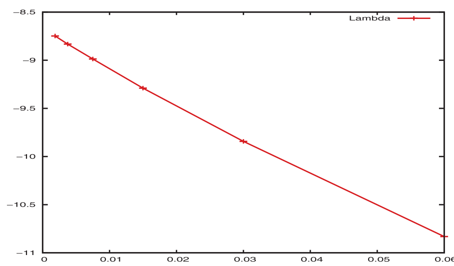

(c) The Lagrange multiplier λ_ε seems to converge as $\varepsilon \searrow 0$.

FIG. 3. *Data corresponding to Figure* 2.

becomes tangential to the line $m\varepsilon$. This indicates that the error resulting from the diffuse interface profile dominates the total approximated error in (35) and that the distance of the zero level sets becomes comparably small. Hence, the level set of φ_ε is already for $\varepsilon < 0.02$ a good approximation of the optimal interface Γ_0.

To complete this picture we also give a plot of the minimal functional values $j_\varepsilon(\varphi_\varepsilon)$ and the Lagrange multipliers λ_ε for the calculated ε values in Figure 3(b) and 3(c). One sees that $(j_\varepsilon(\varphi_\varepsilon))_\varepsilon$ is monotonically decreasing as ε decreases and seems to converge linearly to a specific value, supposedly a minimal value for j_0; compare also Theorem 21. Likewise, $(\lambda_\varepsilon)_\varepsilon$ converges linearly to a limit value λ_0; compare Theorem 22.

To study the influence of the perimeter penalization, we carried out the same calculations for a smaller weighting factor γ. We can control the appearance of fine structures by the choice of γ. As an example, we refer to Figure 1(b), where we used the parameters $\gamma = 0.002$, $\varepsilon = 0.001$. This verifies numerically that the regularization yields a well-posed problem but still gives desired optimal structures. Moreover, the influence of regularization parameters on the fineness of the structure is in accordance to other methods (see, e.g., [9]). For the computation of Figure 1(b) we chose the inner product

$$a_k(\xi, \eta) := \gamma\varepsilon \int_\Omega \nabla\xi \cdot \nabla\eta \,\mathrm{d}x - 2\int_\Omega \mathcal{C}'(\varphi_k)(\xi)\mathcal{E}(\boldsymbol{z}) : \mathcal{E}(\boldsymbol{u}_k)\,\mathrm{d}x,$$

which depends on the current iterate φ_k and which includes second order information of the Ginzburg–Landau energy, as well as of the compliance part. Here, we used $\boldsymbol{u}_k := \boldsymbol{S}(\varphi_k)$ and $\boldsymbol{z} := \boldsymbol{S}'(\varphi_k)\eta \in \boldsymbol{H}^1_D(\Omega)$, which is given as the solution of the

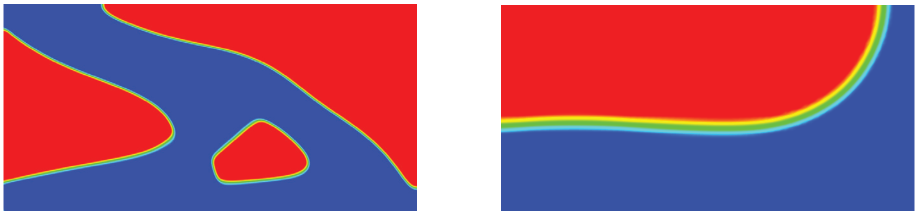

FIG. 4. *Optimal designs including eigenstrain.*

linearized state equation

$$\int_\Omega \mathcal{C}(\varphi_k)\mathcal{E}(\boldsymbol{z}) : \mathcal{E}(\boldsymbol{v})\,\mathrm{d}x = -\int_\Omega \mathcal{C}'(\varphi_k)\eta\mathcal{E}(\boldsymbol{u}_k) : \mathcal{E}(\boldsymbol{v})\,\mathrm{d}x + \int_{\Gamma_g} \boldsymbol{g}\cdot\boldsymbol{v}\,\mathrm{d}s \quad \forall \boldsymbol{v} \in \boldsymbol{H}^1_D(\Omega)\,.$$

3.3. Influence of eigenstrain. In addition to subsection 3.2 we add now eigenstrain to the problem. The influence of the eigenstrain can be seen in Figure 4.

The left figure corresponds to the isotropic eigenstrain $\overline{\mathcal{E}}(\varphi) = \rho\varphi Id$ with $\rho = 0.08$ and the parameters $\varepsilon = 0.01$, $\gamma = 0.5$. For the elasticity constants we took $\lambda_1 = \mu_1 = 5000$ and $\lambda_2 = \mu_2 = 5$, i.e., a strong and a weak material. On the right-hand side the result for an anisotropic eigenstrain $\overline{\mathcal{E}}(\varphi) = \rho\varphi \left(\begin{smallmatrix} -1 & 0 \\ 0 & 1 \end{smallmatrix}\right)$ with $\rho = 0.01$ are presented, where we used the parameters $\varepsilon = 0.04$ and $\gamma = 0.5$. The elastic material constants were assumed to be homogeneous, and we took $\lambda_1 = \mu_1 = \lambda_2 = \mu_2 = 5000$. We notice that the anisotropic eigenstrain leads to a completely different geometry.

3.4. Optimal material distribution within a wing. We now consider a different geometry for the overall container Ω in a three-dimensional setting. This example shows that we can also use different geometries, i.e., different choices of Ω, and work in a three-dimensional setting.

We perform the same optimization strategy as above and optimize the material configuration within a wing of an airplane. This example is to be considered as an outlook on possible applications. One wants to have a composite material in order to obtain a high ratio of stiffness to weight. Hence we use one very stiff material ($\lambda_1 = 5000, \mu_1 = 5000$) and a material representing the light material ($\lambda_2 = 100$, $\mu_2 = 100$). Moreover, we assume that there is no eigenstrain, i.e., $\overline{\mathcal{E}} = 0$. As geometry we use a three-dimensional NACA 0018 airfoil configuration with three holes in it. The configuration can be seen in Figure 5.

The considerations of the previous example have shown that we do not have to choose ε too small in order to obtain the right qualitative behavior, and so we use here $\varepsilon = 0.06$. Moreover, the weighting factor for the Ginzburg–Landau regularization is chosen quite small, i.e., $\gamma = 10^{-4}$. The boundary force $\boldsymbol{g}(x,y,z) = (0, 0.03\sqrt{1-(0.5y)^2}, 0)$ is of elliptic form, which is typical for the lift force acting on an airplane wing; compare, for instance, [24]. Its support is on $\Gamma_g^0 := \{(x,y,z) \in \partial\Omega \mid y > 0\}$. The Dirichlet boundary $\Gamma_D = \{(x,y,z) \in \partial\Omega \mid z = 0\}$ is the part where the wing is attached to the airplane, i.e., the left-hand side in Figure 5(a). The optimized material configuration is shown in Figure 5(a), where the blue material is the stiff material. We also give a picture of the weak material, i.e., the set $\{\varphi_\varepsilon < 0\}$, see Figure 5(b), in order to see the hypersurface separating the two materials. Various cross sections of the wing are displayed in Figure 5(c), where one can also clearly see the three prescribed holes.

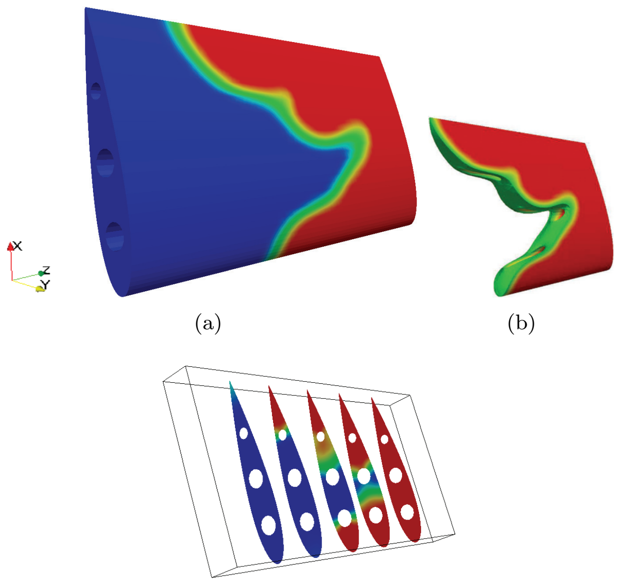

(a) (b)

(c)

FIG. 5. *Optimal material configuration of a NACA* 0018 *airfoil wing with three holes, where blue represents the stiff material.*

4. Proof of existence of optimal solutions. In this section, we want to prove the existence of a minimizer for the optimization problems in the sharp and diffuse interface setting, i.e., Theorems 12 and 17. For this purpose, we start with the following lemma.

LEMMA 24. *Under the assumptions* (A1)–(A5), *the function*

$$F_E : \left\{\varphi \in L^1(\Omega) \mid |\varphi| \leq 1 \ a.e.\ in\ \Omega\right\} \ni \varphi \mapsto \int_\Omega h_\Omega\left(x, \boldsymbol{S}(\varphi)\right) \mathrm{d}x + \int_{\Gamma_g} h_\Gamma\left(s, \boldsymbol{S}\left(\varphi\right)\right) \mathrm{d}s$$

is continuous in $L^1(\Omega)$. *Besides we find that* $\boldsymbol{S} : \{\varphi \in L^1(\Omega) \mid |\varphi| \leq 1 \ a.e.\} \to \boldsymbol{H}^1_D(\Omega)$ *is demicontinuous.*

Proof. Let $(\varphi_n)_{n\in\mathbb{N}} \subset L^1(\Omega)$ be a sequence such that $|\varphi_n| \leq 1$ a.e. in Ω for every $n \in \mathbb{N}$ and $\lim_{n\to\infty} \|\varphi_n - \varphi\|_{L^1(\Omega)} = 0$. In particular, this gives directly $|\varphi| \leq 1$ a.e. in Ω. We now consider any subsequence of $(\varphi_n)_{n\in\mathbb{N}}$ which we will still for simplicity denote by $(\varphi_n)n_{n\in\mathbb{N}}$. Defining $\boldsymbol{u}_n := \boldsymbol{S}(\varphi_n)$ we see that it holds that

$$\int_\Omega \mathcal{C}\left(\varphi_n\right)\left(\mathcal{E}\left(\boldsymbol{u}_n\right) - \overline{\mathcal{E}}\left(\varphi_n\right)\right) : \mathcal{E}\left(\boldsymbol{u}_n\right) \mathrm{d}x = \int_\Omega \boldsymbol{f} \cdot \boldsymbol{u}_n \,\mathrm{d}x + \int_{\Gamma_g} \boldsymbol{g} \cdot \boldsymbol{u}_n \,\mathrm{d}s \quad \forall n \in \mathbb{N}.$$

Thus, by applying the inequalities of Korn, Young, and Hölder and the uniform estimate on the elasticity tensor $\mathcal{C}$, see (4), we obtain that

$$\sup_{n\in\mathbb{N}} \|\boldsymbol{u}_n\|_{\boldsymbol{H}^1(\Omega)} < \infty.$$

And so we find a subsequence $(\boldsymbol{u}_n)_{n\in\mathbb{N}}$, which we denote the same, such that $(\boldsymbol{u}_n)_{n\in\mathbb{N}}$ converges weakly in $\boldsymbol{H}^1(\Omega)$ to some $\boldsymbol{u} \in \boldsymbol{H}^1_D(\Omega)$ as $n \to \infty$. Using the uniform boundedness of the tensor-valued function $\mathcal{C} \in C^{1,1}([-1,1], \mathbb{R}^{d^2\times d^2})$, see assumption (A3), we obtain for any $\boldsymbol{v} \in \boldsymbol{H}^1_D(\Omega)$ the uniform estimate

$$|\mathcal{C}(\varphi_n(x))\,\mathcal{E}(\boldsymbol{v})(x)| \leq C\,|\mathcal{E}(\boldsymbol{v})(x)| \qquad \text{for a.e. } x \in \Omega.$$

Hence, Lebesgue's convergence theorem implies that $(\mathcal{C}(\varphi_n)\mathcal{E}(\boldsymbol{v}))_{n\in\mathbb{N}}$ converges strongly in $L^2(\Omega)^{d\times d}$ to $\mathcal{C}(\varphi)\mathcal{E}(\boldsymbol{v})$. Since $(\mathcal{E}(\boldsymbol{u}_n))_{n\in\mathbb{N}}$ converges additionally weakly in $L^2(\Omega)^{d\times d}$, we obtain that

$$\lim_{n\to\infty}\left|\int_\Omega \mathcal{C}(\varphi_n)\,\mathcal{E}(\boldsymbol{u}_n) : \mathcal{E}(\boldsymbol{v})\,\mathrm{d}x - \int_\Omega \mathcal{C}(\varphi)\,\mathcal{E}(\boldsymbol{u}) : \mathcal{E}(\boldsymbol{v})\,\mathrm{d}x\right| = 0.$$

Similarly, we can deduce from the uniform boundedness of $\overline{\mathcal{E}}$ that

$$\lim_{n\to\infty}\left|\int_\Omega \mathcal{C}(\varphi_n)\,\overline{\mathcal{E}}(\varphi_n) : \mathcal{E}(\boldsymbol{v})\,\mathrm{d}x - \int_\Omega \mathcal{C}(\varphi)\,\overline{\mathcal{E}}(\varphi) : \mathcal{E}(\boldsymbol{v})\,\mathrm{d}x\right| = 0.$$

This leads to

$$\int_\Omega \mathcal{C}(\varphi)\left(\mathcal{E}(\boldsymbol{u}) - \overline{\mathcal{E}}(\varphi)\right) : \mathcal{E}(\boldsymbol{v})\,\mathrm{d}x = \int_\Omega \boldsymbol{f}\cdot\boldsymbol{v}\,\mathrm{d}x + \int_{\Gamma_g} \boldsymbol{g}\cdot\boldsymbol{v}\,\mathrm{d}s \quad \forall \boldsymbol{v} \in \boldsymbol{H}^1_D(\Omega),$$

which yields $\boldsymbol{u} = \boldsymbol{S}(\varphi)$. By applying the same arguments as above for any subsequence of $(\boldsymbol{S}(\varphi_n))_{n\in\mathbb{N}}$, we obtain that every subsequence of $(\boldsymbol{S}(\varphi_n))_{n\in\mathbb{N}}$ has a subsequence $(\boldsymbol{S}(\varphi_{\hat{n}(k)}))_{k\in\mathbb{N}}$ such that $(\boldsymbol{S}(\varphi_{\hat{n}(k)}))_{k\in\mathbb{N}}$ converges weakly in $\boldsymbol{H}^1(\Omega)$ to $\boldsymbol{S}(\varphi) = \boldsymbol{u}$. Since the limit $\boldsymbol{S}(\varphi)$ is unique this implies that the whole sequence converges. This implies then the demicontinuity of $\boldsymbol{S}$ as stated in the lemma.

We are left with proving the continuity of F_E. For this purpose, we take again a sequence $(\varphi_k)_{k\in\mathbb{N}} \subset L^1(\Omega)$ such that $|\varphi_k| \leq 1$ a.e. in Ω and $\lim_{k\to\infty}\|\varphi_k - \varphi\|_{L^1(\Omega)} = 0$. We have already established that this implies the weak convergence of $(\boldsymbol{S}(\varphi_k))_{k\in\mathbb{N}}$ to $\boldsymbol{S}(\varphi)$ in $\boldsymbol{H}^1(\Omega)$. Using the compact embeddings $\boldsymbol{H}^1(\Omega) \hookrightarrow \boldsymbol{L}^2(\Omega)$ and $\boldsymbol{H}^{\frac{1}{2}}(\Gamma_g) \hookrightarrow \boldsymbol{L}^2(\Gamma_g)$ we moreover find that $(\boldsymbol{S}(\varphi_k))_{k\in\mathbb{N}}$ converges strongly in $\boldsymbol{L}^2(\Omega)$ and $(\boldsymbol{S}(\varphi_k)|_{\Gamma_g})_{k\in\mathbb{N}}$ converges strongly in $\boldsymbol{L}^2(\Gamma_g)$. We can now use the continuity of the objective functional stated in assumption (A5), see Remark 4, to obtain $\lim_{k\to\infty} F_E(\varphi_k) = F_E(\varphi)$ and have shown the statement. ∎

Using this lemma, we can show existence of a minimizer for the perimeter penalized sharp interface problem.

Proof of Theorem 12. We use that (18)–(19) is equivalent to $\min_{\varphi\in L^1(\Omega)} j_0(\varphi)$. According to assumption (A5), the objective functional j_0 is bounded from below and hence we may choose a minimizing sequence $(\varphi_k)_{k\in\mathbb{N}}$ for j_0. Thus $P_\Omega(\{\varphi_k = 1\}) = |\mathrm{D}\varphi_k|(\Omega)$ is uniformly bounded. We obtain therefrom and the fact that $\|\varphi_k\|_{L^\infty(\Omega)} \leq 1$ for all $k \in \mathbb{N}$ that $(\varphi_k)_{k\in\mathbb{N}}$ is uniformly bounded in $BV(\Omega)$. As $BV(\Omega)$ embeds compactly into $L^1(\Omega)$, we hence find that $(\varphi_k)_{k\in\mathbb{N}}$ has a subsequence $(\varphi_{k_l})_{l\in\mathbb{N}}$ converging in $L^1(\Omega)$ and pointwise to some limit element $\varphi \in BV(\Omega)$. From the pointwise convergence we obtain $\varphi(x) \in \{\pm 1\}$ for almost every $x \in \Omega$ and the convergence in $L^1(\Omega)$ yields directly $\int_\Omega \varphi\,\mathrm{d}x \leq \beta|\Omega|$. Hence we have $\varphi \in \Phi^0_{ad}$. From Lemma 24, which is given in section 6, we obtain that $\varphi \mapsto \int_\Omega h_\Omega(x, \boldsymbol{S}(\varphi))\,\mathrm{d}x + \int_{\Gamma_g} h_\Gamma(s, \boldsymbol{S}(\varphi))\,\mathrm{d}s$ is continuous in $L^1(\Omega)$. Moreover, the perimeter functional $\varphi \mapsto P_\Omega(\{\varphi = 1\})$ is lower semicontinuous in $L^1(\Omega)$, see [6], and thus we obtain $j_0(\varphi) \leq \liminf_{l\to\infty} j_0(\varphi_{k_l})$. This shows that φ is a minimizer of j_0, and hence $(\varphi, \boldsymbol{S}(\varphi))$ is a minimizer of (18)–(19). ∎

Similarly, we can also show well-posedness of the phase-field problem.

Sketch of a proof of Theorem 17. This is established by using the direct method of the calculus of variations. We choose a minimizing sequence $(\varphi_k)_{k\in\mathbb{N}}$ and using (A5) we obtain that

$$\int_\Omega \left(\frac{\gamma\varepsilon}{2}\left|\nabla\varphi_k\right|^2 + \frac{\gamma}{\varepsilon}\psi(\varphi_k)\right)\,\mathrm{d}x$$

is uniformly bounded. Since $\psi \geq 0$ we obtain that $\int_\Omega(\nabla\varphi_k)^2$ is uniformly bounded and using $\varphi_k \in [-1,1]$ implies that $(\varphi_k)_{k\in\mathbb{N}}$ is uniformly bounded in $\boldsymbol{H}^1(\Omega)$. We hence obtain that a subsequence, which we denote the same, converges weakly in $\boldsymbol{H}^1(\Omega)$, strongly in $\boldsymbol{L}^2(\Omega)$, and a.e. to an $\varphi \in \boldsymbol{H}^1(\Omega)$. We first observe that $\int_\Omega(\frac{\gamma\varepsilon}{2})|\nabla\varphi|^2\,\mathrm{d}x$ is weakly lower semicontinuous. The pointwise convergence of $(\varphi_k)_{k\in\mathbb{N}}$ implies $\int_\Omega \varphi dx \leq \beta|\Omega|$ and $|\varphi| \leq 1$ a.e. In addition we have $\int_\Omega \psi(\varphi_k) \to \int_\Omega \psi(\varphi)$ as $k \to \infty$. This shows that the Ginzburg–Landau energy is weakly lower semicontinuous. The remaining steps can be carried out exactly as in the proof of Theorem 12. We also refer to [31, Theorem 24.1] or [12] for more details. ∎

5. Derivation of the optimality conditions. In this section we will give the proofs of Theorems 13, 18, and 15. We start with showing the differentiability of $t \mapsto (\boldsymbol{S}(\varphi\circ T_t^{-1})\circ T_t)$ at $t=0$ for $T \in \mathcal{T}_{ad}$ and $\varphi \in L^1(\Omega)$, $|\varphi| \leq 1$ and deriving the validity of (23).

LEMMA 25. *Assume* (A1)–(A6). *Let $\varphi \in L^1(\Omega)$ with $|\varphi| \leq 1$ a.e. in Ω and $T \in \mathcal{T}_{ad}$ chosen. We define $\varphi(t) := \varphi\circ T_t^{-1}$ and $\boldsymbol{u}(t) := \boldsymbol{S}(\varphi(t))$ for $|t| \ll 1$. Then $t \mapsto (\boldsymbol{u}(t)\circ T_t) \in \boldsymbol{H}^1_D(\Omega)$ is differentiable at $t=0$ and $\dot{\boldsymbol{u}}[V] := \partial_t|_{t=0}(\boldsymbol{u}(t)\circ T_t) \in \boldsymbol{H}^1_D(\Omega)$ is the unique solution of* (23) *with φ_0 replaced by φ and $\boldsymbol{u}_0$ replaced by $\boldsymbol{u} := \boldsymbol{S}(\varphi)$.*

Proof. The idea is to apply the implicit function theorem for the function $F : (-\tau_0,\tau_0)\times\boldsymbol{H}^1_D(\Omega) \to (\boldsymbol{H}^1_D(\Omega))'$ given by

$$\begin{aligned}F(t,\boldsymbol{u})(\boldsymbol{v}) = &\int_\Omega \mathcal{C}(\varphi)\frac{1}{2}\left(\nabla T_t^{-1}\nabla\boldsymbol{u} + \mathrm{D}\boldsymbol{u}\mathrm{D}T_t^{-1}\right) : \frac{1}{2}(\nabla T_t^{-1}\nabla\boldsymbol{v} + \mathrm{D}\boldsymbol{v}\mathrm{D}T_t^{-1})\det\mathrm{D}T_t\,\mathrm{d}x\\ &- \int_\Omega \mathcal{C}(\varphi)\,\overline{\mathcal{E}}(\varphi) : \frac{1}{2}\left(\nabla T_t^{-1}\nabla\boldsymbol{v} + \mathrm{D}\boldsymbol{v}\mathrm{D}T_t^{-1}\right)\det\mathrm{D}T_t\,\mathrm{d}x\\ &- \int_\Omega \boldsymbol{f}\cdot\left(\boldsymbol{v}\circ T_t^{-1}\right)\,\mathrm{d}x - \int_{\Gamma_g}\boldsymbol{g}\cdot\left(\boldsymbol{v}\circ T_t^{-1}\right)\,\mathrm{d}s,\end{aligned}$$

which is defined for $\tau_0 > 0$ small enough. Using the calculation rules $\nabla(\boldsymbol{v}\circ T_t) = \nabla T_t(\nabla\boldsymbol{v})\circ T_t$, $\mathrm{D}(\boldsymbol{v}\circ T_t) = (\mathrm{D}\boldsymbol{v})\circ T_t\mathrm{D}T_t$ for $\boldsymbol{v} \in \boldsymbol{H}^1(\Omega)$ we can establish

$$\begin{aligned}F(t,\boldsymbol{u}(t)\circ T_t)(\boldsymbol{v}) = &\int_\Omega \mathcal{C}(\varphi(t))\left(\mathcal{E}(\boldsymbol{u}(t)) - \overline{\mathcal{E}}(\varphi(t))\right) : \mathcal{E}(\boldsymbol{v}\circ T_t^{-1})\,\mathrm{d}x\\ &- \int_\Omega \boldsymbol{f}\cdot\left(\boldsymbol{v}\circ T_t^{-1}\right)\,\mathrm{d}x - \int_{\Gamma_g}\boldsymbol{g}\cdot\left(\boldsymbol{v}\circ T_t^{-1}\right)\,\mathrm{d}s = 0,\end{aligned}$$

where we made use of $\boldsymbol{v}\circ T_t^{-1} \in \boldsymbol{H}^1_D(\Omega)$ if $\boldsymbol{v} \in \boldsymbol{H}^1_D(\Omega)$ by the particular choice of

$T \in \mathcal{T}_{ad}$. Besides, $\mathrm{D}_u F(0,\boldsymbol{u}) : \boldsymbol{H}^1_D(\Omega) \to (\boldsymbol{H}^1_D(\Omega))'$ given by

$$\mathrm{D}_u F\left(0,\boldsymbol{u}\right)(\boldsymbol{u})(\boldsymbol{v}) = \int_\Omega \mathcal{C}\left(\varphi\right)\mathcal{E}\left(\boldsymbol{u}\right) : \mathcal{E}\left(\boldsymbol{v}\right)\,\mathrm{d}x \quad \forall \boldsymbol{u},\boldsymbol{v} \in \boldsymbol{H}^1_D(\Omega)$$

is by the Lax–Milgram theorem an isomorphism. And so we can apply the implicit function theorem of Simon [41] to obtain differentiability of $(-\tau_0,\tau_0) \ni t \mapsto (\boldsymbol{u}(t) \circ T_t) \in \boldsymbol{H}^1_D(\Omega)$ at $t = 0$ together with $\dot{\boldsymbol{u}}[V] := \partial_t|_{t=0}(\boldsymbol{u}(t) \circ T_t)$, $\mathrm{D}_u F(0,\boldsymbol{u})\dot{\boldsymbol{u}}[V] = -\partial_t F(0,\boldsymbol{u})$ and obtain therefrom (23). ∎

Now we can directly proof the validity of the optimality system for the sharp interface problem.

Proof of Theorem 13. The formula for the first variation of the perimeter functional can, for instance, be found in [30, section 10.2]. The volume integrals appearing in the objective functional can be differentiated directly by using change of variables. To handle the boundary integrals, we use the calculation rules derived in [22, Chapter 9, section 4.2] to see

$$\partial_t|_{t=0} \int_{T_t(\Gamma_g)} h_\Gamma\left(s,\boldsymbol{u}_0(t)\right)\,\mathrm{d}s = \partial_t|_{t=0} \int_{\Gamma_g} h_\Gamma\left(T_t(s),\boldsymbol{u}_0(t)\circ T_t\right)\omega_t\,\mathrm{d}s,$$

where $\omega_t = |\det \mathrm{D}T_t \mathrm{D}T_t^{-T}\boldsymbol{n}|$, $\boldsymbol{u}_0(t) := \boldsymbol{S}(\varphi_0 \circ T_t^{-1})$. The derivative of ω_t with respect to t at can be calculated by $\partial_t|_{t=0}\omega_t = \operatorname{div} V(0) - \boldsymbol{n}\cdot\nabla V(0)\boldsymbol{n}$. For more details we refer to [22]. And so we arrive at

$$\begin{aligned}\partial_t|_{t=0} \int_{T_t(\Gamma_g)} h_\Gamma\left(s,\boldsymbol{u}_0(t)\right)\,\mathrm{d}s = \int_{\Gamma_g} &\mathrm{D}h_\Gamma\left(s,\boldsymbol{u}_0\right)\left(V(0),\dot{\boldsymbol{u}}_0\left[V\right]\right) \\ &+ h_\Gamma\left(s,\boldsymbol{u}_0\right)\left(\operatorname{div} V(0) - \boldsymbol{n}\cdot\nabla V(0)\boldsymbol{n}\right)\,\mathrm{d}s,\end{aligned}$$

where $\dot{\boldsymbol{u}}_0[V] := \partial_t|_{t=0}(\boldsymbol{u}_0(t) \circ T_t)$ is already determined by Lemma 25.

We will now discuss the existence of a Lagrange multiplier for the integral constraint. First we may assume without loss of generality that $\int_\Omega \varphi_0\,\mathrm{d}x = \beta|\Omega|$; otherwise any transformation $T \in \mathcal{T}_{ad}$ will yield admissible comparison functions $\varphi_0 \circ T_t^{-1} \in \Phi^0_{ad}$ for $|t| \ll 1$ and in this case $\lambda_0 = 0$ is the desired Lagrange multiplier. Considering the case $\int_\Omega \varphi_0\,\mathrm{d}x = \beta|\Omega|$, we choose some $W \in \mathcal{V}_{ad}$ with associated transformation $S \in \mathcal{T}_{ad}$ such that $\int_\Omega \varphi_0 \operatorname{div} W(0)\,\mathrm{d}x = -1$ and define $g : [-t_0,t_0] \times [-s_0,s_0] \to \mathbb{R}$ by $g(t,s) := -\int_\Omega \varphi_0 \circ T_t^{-1} \circ S_s^{-1}\,\mathrm{d}x + \beta|\Omega|$ for $s_0, t_0 > 0$ small enough. Direct calculation yields $\partial_s|_{s=0} g(0,s) = -\int_\Omega \varphi_0 \operatorname{div} W(0)\,\mathrm{d}x = 1 \neq 0$. And so we apply the implicit function theorem to obtain $s \in C^1((-\tau_0,\tau_0),\mathbb{R})$ such that $g(t,s(t)) = 0$ for $|t| \ll 1$, $s'(0) = -\partial_s|_{s=0} g(0,s)^{-1}\partial_t|_{t=0} g(t,0) = -\partial_t|_{t=0} g(t,0)$. Hence $\varphi_0 \circ T_t^{-1} \circ S_{s(t)}^{-1} \in \Phi^0_{ad}$ for $|t| \ll 1$ and thus $\partial_t|_{t=0} j_0(\varphi_0 \circ (S_{s(t)} \circ T_t)^{-1}) = 0$. One can then establish that

$$\begin{aligned}0 &= \partial_t|_{t=0} j_0\left(\varphi_0 \circ (S_{s(t)} \circ T_t)^{-1}\right) = \partial_s|_{s=0} j_0\left(\varphi_0 \circ S_s^{-1}\right) s'(0) + \partial_t|_{t=0} j_0\left(\varphi_0 \circ T_t^{-1}\right) \\ &= \lambda_0 \int_\Omega \varphi_0 \operatorname{div} V(0)\,\mathrm{d}x + \partial_t|_{t=0} j_0\left(\varphi_0 \circ T_t^{-1}\right),\end{aligned}$$

where we defined $\lambda_0 := \partial_s|_{s=0} j_0(\varphi_0 \circ S_s^{-1})$. As we chose $\int_\Omega \varphi_0 \operatorname{div} W(0) = -1 < 0$ we have that $\int_\Omega \varphi_0 \circ S_s^{-1}\,\mathrm{d}x \leq \beta|\Omega|$, and hence $\varphi_0 \circ S_s^{-1} \in \Phi^0_{ad}$, for $0 < s \ll 1$. This shows $\lambda_0 \geq 0$ and yields in particular that λ_0 is a Lagrange multiplier. For more details we refer to [31, Lemma 7.5]; see also [29]. ∎

Similarly, we directly establish the corresponding optimality system for the phase field problems.

Proof of Theorem 18. We follow the lines of the proof of Theorem 13. The differential of the terms from the Ginzburg–Landau energy can be treated by direct calculation; compare, for instance, [31, Lemma 7.5]. ∎

We now want to outline the main steps of proving Theorem 15. Essentially, this can be shown by using basic facts such as integration by parts and the chain rule. This calculation has been carried out in detail, for instance, in [31, Theorem 25.3], and we outline in the following the main ideas and steps.

Sketch of proof of Theorem 15. We start by using [5, 10.2] to see that under the stated regularity assumptions it holds with the help of the generalized Gauss-Green theorem that

$$\int_\Omega (\operatorname{div} V(0) - \nu \cdot \nabla V(0)\nu) \,\mathrm{d}\,|\mathrm{D}\chi_{E_0}| = \int_{\partial E_0 \cap \Omega} \kappa V(0) \cdot \nu.$$

Additionally, we find by the stated regularity assumptions on Γ_g directly

$$\int_{\Gamma_g} h_\Gamma(s, \boldsymbol{u}_0) (\operatorname{div} V(0) - \nu \cdot \nabla V(0)\nu) \,\mathrm{d}s = \int_{\Gamma_g} h_\Gamma(s, \boldsymbol{u}_0) \operatorname{div}_{\Gamma_g} V(0) \mathrm{d}s.$$

In the next step, we multiply the strong formulation of the linearized equation (23) in each phase with the adjoint variable, integrate, and perform several integration by parts. We then simplify the resulting equation with the identities resulting from multiplying the strong formulation of the state equation for $\boldsymbol{u}_0$ with $\mathrm{D}\boldsymbol{q}_0 V(0)$ and from multiplying the adjoint equation with $\mathrm{D}\boldsymbol{u}_0 V(0)$ to find that after integration

(36)
$$\begin{aligned}
&\int_\Omega \mathcal{C}(\varphi_0)\mathcal{E}(\dot{\boldsymbol{u}}_0[V]) : \mathcal{E}(\boldsymbol{q}_0) \,\mathrm{d}x \\
&\quad= \int_\Omega -\mathcal{C}(\varphi_0)\frac{1}{2} (\nabla(\mathrm{D}\boldsymbol{u}_0)V(0) + \mathrm{D}(\mathrm{D}\boldsymbol{u}_0)V(0)) : \mathcal{E}(\boldsymbol{q}_0) \\
&\qquad - \mathcal{C}(\varphi_0) \left(\mathcal{E}(\boldsymbol{u}_0) - \overline{\mathcal{E}}(\varphi_0)\right) : \frac{1}{2}(\nabla(\mathrm{D}\boldsymbol{q}_0)V(0) + \mathrm{D}(\mathrm{D}\boldsymbol{q}_0)V(0)) \\
&\qquad - \mathcal{C}(\varphi_0) \left(\mathcal{E}(\boldsymbol{u}_0) - \overline{\mathcal{E}}(\varphi_0)\right) : \mathcal{E}(\boldsymbol{q}_0) \operatorname{div} V(0) \,\mathrm{d}x \\
&\qquad + \int_\Gamma \left[\mathcal{C}(\varphi_0) \left(\mathcal{E}(\boldsymbol{u}_0) - \overline{\mathcal{E}}(\varphi_0)\right) \nu \cdot \mathrm{D}\boldsymbol{q}_0 V(0)\right]_\Gamma + \left[\mathcal{C}(\varphi_0)\mathcal{E}(\boldsymbol{q}_0)\nu \cdot \mathrm{D}\boldsymbol{u}_0 V(0)\right]_\Gamma \,\mathrm{d}x \\
&\qquad + \int_\Omega \mathrm{D}_u h_\Omega(x, \boldsymbol{u}_0) (\mathrm{D}\boldsymbol{u}_0 V(0)) \,\mathrm{d}x + \int_{\Gamma_g} \mathrm{D}_u h_\Gamma(x, \boldsymbol{u}_0) (\mathrm{D}\boldsymbol{u}_0 V(0)) \,\mathrm{d}x.
\end{aligned}$$

Substituting

$$\begin{aligned}
&\int_\Omega \mathcal{C}(\varphi_0) \left(\mathcal{E}(\boldsymbol{u}_0) - \overline{\mathcal{E}}(\varphi_0)\right) : \mathcal{E}(\boldsymbol{q}_0) \operatorname{div} V(0) \,\mathrm{d}x \\
&\quad= -\int_\Omega \nabla(\mathcal{C}(\varphi_0) \left(\mathcal{E}(\boldsymbol{u}_0) - \overline{\mathcal{E}}(\varphi_0)\right) : \mathcal{E}(\boldsymbol{q}_0)) \cdot V(0) \,\mathrm{d}x \\
&\qquad + \int_\Gamma \left[\mathcal{C}(\varphi_0) \left(\mathcal{E}(\boldsymbol{u}_0) - \overline{\mathcal{E}}(\varphi_0)\right) : \mathcal{E}(\boldsymbol{q}_0)(V(0) \cdot \nu)\right]_\Gamma \,\mathrm{d}x
\end{aligned}$$

into (36) we have

(37)
$$\begin{aligned}
&\int_\Omega \mathcal{C}(\varphi_0)\mathcal{E}(\dot{\boldsymbol{u}}_0[V]) : \mathcal{E}(\boldsymbol{q}_0)\,\mathrm{d}x \\
&\quad = -\int_\Gamma [\mathcal{C}(\varphi_0)\left(\mathcal{E}(\boldsymbol{u}_0) - \overline{\mathcal{E}}(\varphi_0)\right) : \mathcal{E}(\boldsymbol{q}_0)]_\Gamma (V(0)\cdot\nu)\,\mathrm{d}x \\
&\qquad + \int_\Gamma \left[\mathcal{C}(\varphi_0)\left(\mathcal{E}(\boldsymbol{u}_0) - \overline{\mathcal{E}}(\varphi_0)\right)\nu\cdot \mathrm{D}\boldsymbol{q}_0 V(0)\right]_\Gamma + [\mathcal{C}(\varphi_0)\mathcal{E}(\boldsymbol{q}_0)\nu\cdot \mathrm{D}\boldsymbol{u}_0 V(0)]_\Gamma\,\mathrm{d}x \\
&\qquad + \int_\Omega \mathrm{D}_u h_\Omega(x,\boldsymbol{u}_0)\left(\mathrm{D}\boldsymbol{u}_0 V(0)\right)\,\mathrm{d}x + \int_{\Gamma_g} \mathrm{D}_u h_\Gamma(x,\boldsymbol{u}_0)\left(\mathrm{D}\boldsymbol{u}_0 V(0)\right)\,\mathrm{d}x.
\end{aligned}$$

On the other hand, inserting $\dot{\boldsymbol{u}}_0[V]$ as a test function in the adjoint state system we obtain

$$\begin{aligned}
\int_\Omega \mathcal{C}(\varphi_0)\mathcal{E}(\boldsymbol{q}_0) : \mathcal{E}(\dot{\boldsymbol{u}}_0[V])\,\mathrm{d}x = &\int_\Omega \mathrm{D}_u h_\Omega(x,\boldsymbol{u}_0)\left(\dot{\boldsymbol{u}}_0[V]\right)\,\mathrm{d}x \\
&+ \int_{\Gamma_g} \mathrm{D}_u h_\Gamma(x,\boldsymbol{u}_0)\,\dot{\boldsymbol{u}}_0[V]\,\mathrm{d}x.
\end{aligned} \tag{38}$$

Thus, combining (37) and (38) we obtain

$$\begin{aligned}
&\int_\Omega \mathrm{D}_u h_\Omega(x,\boldsymbol{u}_0)\dot{\boldsymbol{u}}_0[V]\,\mathrm{d}x + \int_{\Gamma_g} \mathrm{D}_u h_\Gamma(x,\boldsymbol{u}_0)\,\dot{\boldsymbol{u}}_0[V]\,\mathrm{d}x \\
&\quad = \int_\Gamma \left[-\mathcal{C}(\varphi_0)\left(\mathcal{E}(\boldsymbol{u}_0) - \overline{\mathcal{E}}(\varphi_0)\right) : \mathcal{E}(\boldsymbol{q}_0) + \mathcal{C}(\varphi_0)\left(\mathcal{E}(\boldsymbol{u}_0) - \overline{\mathcal{E}}(\varphi_0)\right)\nu\cdot\partial_\nu \boldsymbol{q}_0\right. \\
&\qquad\quad \left. + \mathcal{C}(\varphi_0)\mathcal{E}(\boldsymbol{q}_0)\nu\cdot\partial_\nu\boldsymbol{u}_0\right]_\Gamma (V(0)\cdot\nu)\,\mathrm{d}x \\
&\qquad + \int_\Omega \mathrm{D}_u h_\Omega(x,\boldsymbol{u}_0)\left(\mathrm{D}\boldsymbol{u}_0 V(0)\right)\,\mathrm{d}x + \int_{\Gamma_g} \mathrm{D}_u h_\Gamma(x,\boldsymbol{u}_0)\left(\mathrm{D}\boldsymbol{u}_0 V(0)\right)\,\mathrm{d}x.
\end{aligned}$$

Using $\mathrm{D}(h_\Gamma(x,\boldsymbol{u}_0(x))) = \mathrm{D}_{\Gamma_g}(h_\Gamma(x,\boldsymbol{u}_0(x))) + \partial_{\boldsymbol{n}}(h_\Gamma(x,\boldsymbol{u}_0(x)))\cdot\boldsymbol{n}$ we end up with

(39)
$$\begin{aligned}
&\partial_t|_{t=0} j_0\left(\varphi_0\circ T_t^{-1}\right) \\
&\quad = \int_\Gamma \left[-\mathcal{C}(\varphi_0)\left(\mathcal{E}(\boldsymbol{u}_0) - \overline{\mathcal{E}}(\varphi_0)\right) : \mathcal{E}(\boldsymbol{q}_0)\right. \\
&\qquad\quad \left. + \mathcal{C}(\varphi_0)\left(\mathcal{E}(\boldsymbol{u}_0) - \overline{\mathcal{E}}(\varphi_0)\right)\nu\cdot\partial_\nu\boldsymbol{q}_0 + \mathcal{C}(\varphi_0)\mathcal{E}(\boldsymbol{q}_0)\nu\cdot\partial_\nu\boldsymbol{u}_0\right]_\Gamma (V(0)\cdot\nu)\,\mathrm{d}x \\
&\qquad + \int_\Omega \mathrm{D}h_\Omega(x,\boldsymbol{u}_0)\left(V(0),\mathrm{D}\boldsymbol{u}_0 V(0)\right)\,\mathrm{d}x + \int_{\Gamma_g} \mathrm{D}h_\Gamma(x,\boldsymbol{u}_0)\left(V(0),\mathrm{D}\boldsymbol{u}_0 V(0)\right)\,\mathrm{d}x \\
&\qquad + \int_\Omega h_\Omega(x,\boldsymbol{u}_0)\,\mathrm{div}\,V(0)\,\mathrm{d}x + \int_{\Gamma_g} h_\Gamma(x,\boldsymbol{u}_0)\,\mathrm{div}_{\,\partial\Omega}V(0)\,\mathrm{d}x + \gamma c_0\int_\Gamma \kappa(V(0)\cdot\nu) \\
&\quad = \int_\Gamma \left[-\mathcal{C}(\varphi_0)\left(\mathcal{E}(\boldsymbol{u}_0) - \overline{\mathcal{E}}(\varphi_0)\right) : \mathcal{E}(\boldsymbol{q}_0) + \mathcal{C}(\varphi_0)\left(\mathcal{E}(\boldsymbol{u}_0) - \overline{\mathcal{E}}(\varphi_0)\right)\nu\cdot\partial_\nu\boldsymbol{q}_0\right. \\
&\qquad\quad \left. + \mathcal{C}(\varphi_0)\mathcal{E}(\boldsymbol{q}_0)\nu\cdot\partial_\nu\boldsymbol{u}_0 + h_\Omega(x,\boldsymbol{u}_0)\right]_\Gamma (V(0)\cdot\nu) + \gamma c_0\kappa(V(0)\cdot\nu)\,\mathrm{d}x.
\end{aligned}$$

For the last step we made use of the tangential Stokes formula; see [22, Chapter 9, section 5.5]. Thus, using (20) and (39) we find

$$
\begin{aligned}
&\int_\Gamma \left[-\mathcal{C}(\varphi_0)\left(\mathcal{E}(\boldsymbol{u}_0)-\overline{\mathcal{E}}\left(\varphi_0\right)\right):\mathcal{E}(\boldsymbol{q}_0)+\mathcal{C}(\varphi_0)\left(\mathcal{E}\left(\boldsymbol{u}_0\right)-\overline{\mathcal{E}}\left(\varphi_0\right)\right)\nu\cdot\partial_\nu\boldsymbol{q}_0\right.\\
&\qquad\left.+\,\mathcal{C}(\varphi_0)\mathcal{E}\left(\boldsymbol{q}_0\right)\nu\cdot\partial_\nu\boldsymbol{u}_0+h_\Omega\left(x,\boldsymbol{u}_0\right)\right]_\Gamma\left(V(0)\cdot\nu\right)+\gamma c_0\kappa(V(0)\cdot\nu)\,\mathrm{d}x\\
&\quad=-\lambda_0\int_\Omega\varphi_0\operatorname{div}V(0)\,\mathrm{d}x=-2\lambda_0\int_\Gamma V(0)\cdot\nu\,\mathrm{d}x.
\end{aligned}
\tag{40}
$$

Since (40) is fulfilled for any $V\in\mathcal{V}_{ad}$ we obtain the pointwise relation (24) on Γ_0. ∎

6. Proof of the convergence results. In this section we want to prove the convergence results stated in Theorems 20 and 22. First, we want to give a proof of the Γ-convergence result of Theorem 20. Using Lemma 24, we can show Theorem 20 by applying known results concerning Γ-convergence of the Ginzburg–Landau energy.

Proof of Theorem 20. By [16, 35] we obtain that the Ginzburg–Landau energy $E_\varepsilon : L^1(\Omega)\to\overline{\mathbb{R}}$, which is given by

$$
E_\varepsilon\left(\varphi\right):=\begin{cases}\int_\Omega \frac{1}{\varepsilon}\psi\left(\varphi\right)+\frac{\varepsilon}{2}\left|\nabla\varphi\right|^2\,\mathrm{d}x & \text{if } \varphi\in H^1(\Omega),\\ +\infty & \text{otherwise,}\end{cases}
$$

Γ-converges as $\varepsilon\searrow 0$ in $L^1(\Omega)$ to

$$
E_0 : L^1(\Omega)\ni\varphi\mapsto\begin{cases}c_0P_\Omega\left(\{\varphi=1\}\right) & \text{if } \varphi\in BV(\Omega,\{\pm1\}),\\ +\infty & \text{else.}\end{cases}
$$

We rewrite the reduced objective functional in the following form: $j_\varepsilon=\gamma E_\varepsilon+F_E+I_K$, where $I_K(\varphi):=0$ if $\varphi\in K$ and $I_K(\varphi)=+\infty$ if $\varphi\in L^1(\Omega)\setminus K$ with $K:=\{\varphi\in L^1(\Omega)\mid\int_\Omega\varphi\,\mathrm{d}x\le\beta|\Omega|\}$. Using the constructions of Modica [35] one obtains that equality and hence also inequality constraints can be treated in the Γ–convergence of E_ε. This implies that $\gamma E_\varepsilon+I_K$ Γ-converges to γE_0+I_K. Making use of Lemma 24, we find that F_E is a continuous function in $L^1(\Omega)$, and so j_ε is the energy $\gamma E_\varepsilon+I_K$ plus some functional which is continuous in $L^1(\Omega)$. Consequently, by standard results for Γ-convergence, see, for instance, Proposition 6.21 in [20], we find that $(j_\varepsilon)_{\varepsilon>0}$ Γ-converges in $L^1(\Omega)$ to j_0, since $j_0(\varphi)=(\gamma E_0+I_K)(\varphi)+F_E(\varphi)$. This proves the statement. ∎

Now we want to prove the convergence of the equations of the first variation.

Proof of Theorem 22. The result of Corollary 21 yields directly the existence of a subsequence of $(\varphi_\varepsilon)_{\varepsilon>0}$ converging in $L^1(\Omega)$ to a minimizer φ_0 of j_0 such that $\lim_{\varepsilon\searrow0}j_\varepsilon(\varphi_\varepsilon)=j_0(\varphi_0)$. By Lemma 24, this implies the weak convergence of $(\boldsymbol{u}_\varepsilon)_{\varepsilon>0}$ to $\boldsymbol{u}_0=\boldsymbol{S}(\varphi_0)$ in $\boldsymbol{H}^1(\Omega)$ as $\varepsilon\searrow 0$.

Now we recall that $\dot{\boldsymbol{u}}_\varepsilon[V] \in \boldsymbol{H}^1_D(\Omega)$ is given as the solution of

$$\int_\Omega \mathcal{C}(\varphi_\varepsilon)\mathcal{E}(\dot{\boldsymbol{u}}_\varepsilon[V]) : \mathcal{E}(\boldsymbol{v})\,\mathrm{d}x = \boldsymbol{R}_\varepsilon(\boldsymbol{v}) \quad \forall \boldsymbol{v} \in \boldsymbol{H}^1_D(\Omega), \tag{41}$$

where $\boldsymbol{R}_\varepsilon \in (\boldsymbol{H}^1_D(\Omega))'$ is given by

$$\begin{aligned}\boldsymbol{R}_\varepsilon(\boldsymbol{v}) := \int_\Omega & \mathcal{C}(\varphi_\varepsilon)\frac{1}{2}\left(\mathrm{D}\boldsymbol{u}_\varepsilon \mathrm{D}V(0) + \nabla V(0)\nabla \boldsymbol{u}_\varepsilon\right) : \mathcal{E}(\boldsymbol{v}) \\ & + \mathcal{C}(\varphi_\varepsilon)\left(\mathcal{E}(\boldsymbol{u}_\varepsilon) - \overline{\mathcal{E}}\left(\varphi_\varepsilon\right)\right) : \frac{1}{2}(\nabla V(0)\nabla \boldsymbol{v} + \mathrm{D}\boldsymbol{v}\mathrm{D}V(0)) \\ & - \mathcal{C}(\varphi_\varepsilon)\left(\mathcal{E}(\boldsymbol{u}_\varepsilon) - \overline{\mathcal{E}}\left(\varphi_\varepsilon\right)\right) : \mathcal{E}(\boldsymbol{v})\,\mathrm{div}\, V(0)\,\mathrm{d}x \\ & - \int_\Omega \boldsymbol{f}\cdot \mathrm{D}\boldsymbol{v}V(0)\,\mathrm{d}x - \int_{\Gamma_g} \boldsymbol{g}\cdot \mathrm{D}\boldsymbol{v}V(0)\,\mathrm{d}s.\end{aligned}$$

Since $(\boldsymbol{u}_\varepsilon)_{\varepsilon>0}$ is uniformly bounded in $\boldsymbol{H}^1(\Omega)$, $\|\varphi_\varepsilon\|_{L^\infty(\Omega)} \le 1$ and using the uniform estimate on the elasticity tensor and the eigenstrain given by assumptions (A3) and (A4) we can deduce that $\sup_{\varepsilon>0}\|\boldsymbol{R}_\varepsilon\|_{(\boldsymbol{H}^1_D(\Omega))'} < \infty$. And so we find by Korn's inequality from (41) that $\sup_{\varepsilon>0}\|\dot{\boldsymbol{u}}_\varepsilon[V]\|_{\boldsymbol{H}^1(\Omega)} \le C$. This yields the existence of a subsequence, which will be denoted by the same, such that $(\dot{\boldsymbol{u}}_\varepsilon[V])_{\varepsilon>0}$ converges weakly in $\boldsymbol{H}^1(\Omega)$ to $\boldsymbol{w} \in \boldsymbol{H}^1_D(\Omega)$. Following the arguments of the proof of Lemma 24 we see that the limit element $\boldsymbol{w}$ of $(\dot{\boldsymbol{u}}_\varepsilon[V])_{\varepsilon>0}$ fulfills (23). Hence, by definition of $\dot{\boldsymbol{u}}_0[V]$, see Theorem 13, we get $\boldsymbol{w} = \dot{\boldsymbol{u}}_0[V]$. In particular, we can deduce by the embedding theorems that both $(\boldsymbol{u}_\varepsilon)_{\varepsilon>0}$ and $(\dot{\boldsymbol{u}}_\varepsilon[V])_{\varepsilon>0}$ converge strongly in $\boldsymbol{L}^2(\Omega)$ and $\boldsymbol{L}^2(\Gamma_g)$. And so we obtain by the continuous differentiability of the objective functional, see Remark 5, that

(42)
$$\begin{aligned}\lim_{\varepsilon\searrow 0}\Bigg[\int_\Omega & \left[\mathrm{D}h_\Omega\left(x,\boldsymbol{u}_\varepsilon\right)\left(V(0),\dot{\boldsymbol{u}}_\varepsilon\left[V\right]\right) + h_\Omega\left(x,\boldsymbol{u}_\varepsilon\right)\,\mathrm{div}\, V(0)\right]\,\mathrm{d}x \\ & + \int_{\Gamma_g}\left[\mathrm{D}h_\Gamma\left(s,\boldsymbol{u}_\varepsilon\right)\left(V(0),\dot{\boldsymbol{u}}_\varepsilon\left[V\right]\right) + h_\Gamma\left(s,\boldsymbol{u}_\varepsilon\right)\left(\,\mathrm{div}\, V(0) - \boldsymbol{n}\cdot\nabla V(0)\boldsymbol{n}\right)\right]\,\mathrm{d}s\Bigg] \\ = \int_\Omega & \left[\mathrm{D}h_\Omega\left(x,\boldsymbol{u}_0\right)\left(V(0),\dot{\boldsymbol{u}}_0\left[V\right]\right) + h_\Omega\left(x,\boldsymbol{u}_0\right)\,\mathrm{div}\, V(0)\right]\,\mathrm{d}x \\ & + \int_{\Gamma_g}\left[\mathrm{D}h_\Gamma\left(s,\boldsymbol{u}_0\right)\left(V(0),\dot{\boldsymbol{u}}_0\left[V\right]\right) + h_\Gamma\left(s,\boldsymbol{u}_0\right)\left(\,\mathrm{div}\, V(0) - \boldsymbol{n}\cdot\nabla V(0)\boldsymbol{n}\right)\right]\,\mathrm{d}s.\end{aligned}$$

Analogously as in [29] we can apply the Reshetnyak continuity theorem to deduce

$$\begin{aligned}&\lim_{\varepsilon\searrow 0}\left[\int_\Omega \left(\frac{\gamma\varepsilon}{2}\left|\nabla\varphi_\varepsilon\right|^2 + \frac{\gamma}{\varepsilon}\psi\left(\varphi_\varepsilon\right)\right)\,\mathrm{div}\, V(0) - \gamma\varepsilon\nabla\varphi_\varepsilon\cdot\nabla V(0)\nabla\varphi_\varepsilon\,\mathrm{d}x\right] \\ &\quad = \gamma c_0\int_\Omega\left(\,\mathrm{div}\, V(0) - \nu\cdot\nabla V(0)\nu\right)\,\mathrm{d}\left|\mathrm{D}\chi_{E_0}\right|.\end{aligned} \tag{43}$$

Plugging those results together we end up with $\lim_{\varepsilon\searrow 0}\partial_t|_{t=0}j_\varepsilon(\varphi_\varepsilon\circ T_t^{-1}) = \partial_t|_{t=0}j_0$ $(\varphi_0\circ T_t^{-1})$. As in [29] we can find some $V\in\mathcal{V}_{ad}$ such that $\int_\Omega\varphi_0\,\mathrm{div}\, V(0)\,\mathrm{d}x > 0$ if we assume $|\{\varphi_0 = 1\}| > 0$. Thus we have

$$\lim_{\varepsilon\searrow 0} -\lambda_\varepsilon\int_\Omega\varphi_\varepsilon\,\mathrm{div}\, V(0)\,\mathrm{d}x = \lim_{\varepsilon\searrow 0}\partial_t|_{t=0}j_\varepsilon\left(\varphi_\varepsilon\circ T_t^{-1}\right) = \partial_t|_{t=0}j_0\left(\varphi_0\circ T_t^{-1}\right),$$

wherefrom we obtain that $(\lambda_\varepsilon)_{\varepsilon>0}$ converges to some $\lambda_0 \geq 0$. Besides, this directly yields that $\lambda_0 \geq 0$ fulfills (20) and thus is a Lagrange multiplier associated to the integral constraint. This finally proves the statement. ∎

7. Conclusions. We have shown that the proposed phase field approach leads to an optimal control problem for which the existence of a solution can be shown. The problem can be reformulated in such a way that a reduced objective functional has to be minimized. The latter Γ-converges in $L^1(\Omega)$ as the thickness of the interface tends to zero to a functional describing a sharp interface formulation of the problem. We have shown that certain first order optimality conditions for the phase field problem can be deduced by geometric variations. As the minimizers converge, the obtained optimality conditions also converge to a system, which is a necessary optimality condition for the sharp interface problem. Besides, this optimality system for the sharp interface problem can be derived in the general setting of functions of bounded variations.

Assuming additional regularity assumptions on the minimizing set and the data, it can be shown that the obtained conditions are equivalent to results that were already obtained in literature by classical shape calculus and also by formal asymptotics from the phase field model. Thus we have delivered a rigorous proof for the convergence results that were already predicted by formal asymptotics in [12]. Moreover we use a general objective functional. However, in [12] the state constraints can be ε-dependent. To be precise, an ersatz material approach is used, where the stiffness of the ersatz material scales like ε^2 and thus vanishes as $\varepsilon \searrow 0$. This is not done in our work, but possible generalizations for reasonable objective functionals in the spirit of [28, 29] may be possible. This means that convergence of minimizers could possibly be shown, but we expect that again certain growth conditions on the convergence of the minimizers play a role, where this rate has to be consistent with the ε-scaling of the ersatz material.

We presented numerical simulations which were obtained with the help of a projected gradient type method which showed that the proposed phase field approach works well in two and three spatial dimensions.

REFERENCES

[1] G. Allaire, C. Dapogny, G. Delgado, and G. Michailidis, *Multi-phase structural optimization via a level set method*, ESAIM Control Optim Calc. Var., 20 (2014), pp. 576–611.

[2] G. Allaire and F. Jouve, *A level-set method for vibration and multiple loads structural optimization*, Comput. Methods Appl. Mech. Engrg., 194 (2005), pp. 3269–3290.

[3] G. Allaire, F. Jouve, and A.-M. Toader, *Structural optimization using sensitivity analysis and a level-set method*, J. Comput. Phys., 194 (2004), pp. 363–393.

[4] G. Allaire, F. Jouve, and N. Van Goethem, *Damage evolution in brittle materials by shape and topological sensitivity analysis*, J. Comput. Phys., 230 (2011), pp. 5010–5044.

[5] L. Ambrosio and G. Buttazzo, *An optimal design problem with perimeter penalization*, Calc. Var. Partial Differential Equations, 1 (1993), pp. 55–69.

[6] L. Ambrosio, N. Fusco, and D. Pallara, *Functions of Bounded Variation and Free Discontinuity Problems*, Clarendon Press, Oxford, 2000.

[7] J. Barrett, R. Nürnberg, and V. Styles, *Finite element approximation of a phase field model for void electromigration*, SIAM J. Numer. Anal., 42 (2004), pp. 738–772.

[8] M. Bendsøe, R. Haber, and C. Jog, *A new approach to variable-topology shape design using a constraint on perimeter*, Struct. Multidiscip. Optim., 11 (1996), pp. 1–12.

[9] M. Bendsøe and O. Sigmund, *Topology Optimization: Theory, Methods and Applications*, Springer, New York, 2003.

[10] M. Bergounioux, K. Ito, and K. Kunisch, *Primal-dual strategy for constrained optimal control problems*, SIAM J. Control Optim., 37 (1999), pp. 1176–1194.

[11] C. Bernardi and O. Pironneau, *Sensitivity of Darcy's law to discontinuities*, Chin. Ann. Math. Ser. B, 24 (2003), pp. 205–214.
[12] L. Blank, H. Farshbaf-Shaker, H. Garcke, and V. Styles, *Relating phase field and sharp interface approaches to structural topology optimization*, ESAIM Control Optim. Calc. Var., 20 (2014), pp. 1024–1058.
[13] L. Blank, M. Farshbaf-Shaker, H. Garcke, C. Rupprecht, and V. Styles, *Multi-material phase field approach to structural topology optimization*, in Trends in PDE Constrained Optimization, G. Leugering, P. Benner, S. Engell, A. Griewank, H. Harbrecht, M. Hinze, R. Rannacher, and S. Ulbrich, eds., Internat. Ser. Numer. Math. 165, Birkhäuser, Basel, 2014, pp. 231–246.
[14] L. Blank, H. Garcke, L. Sarbu, T. Srisupattarawanit, V. Styles, and A. Voigt, *Phase-field approaches to structural topology optimization*, in Constrained Optimization and Optimal Control for Partial Differential Equations, G. Leugering, S. Engell, M. Hinze, R. Rannacher, V. Schulz, V. Ulbrich, and S. Ulbrich, eds., Internat. Ser. Numer Math. 160, Birkhäuser, Basel 2012, pp. 245–256.
[15] L. Blank and C. Rupprecht, *An Extension of the Projected Gradient Method to a Banach Space Setting with Application in Sstructural Ttopology Optimization*, preprint, arXiv:1503.03783v2.
[16] J. F. Blowey and C. M. Elliott, *The Cahn–Hilliard gradient theory for phase separation with non-smooth free energy Part* I: *Mathematical analysis*, European J. Appl. Math., 2 (1991), pp. 233–280.
[17] B. Bourdin and A. Chambolle, *Design-dependent loads in topology optimization*, ESAIM Control Optim. Calc. Var., 9 (2003), pp. 19–48.
[18] D. Braess, *Finite Elemente*, Springer, New York, 1997.
[19] P. Ciarlet, *Three-Dimensional Elasticity*, Stud. Math. Appl. 1, Elsevier Science, New York, 1988.
[20] G. Dal Maso, *An Introduction to* Γ*-convergence*, Progress in Nonlinear Differential Equations and Their Applications, Birkhäuser, Basel, 1993.
[21] M. Delfour and J. Zolésio, *Shapes and geometries: Analysis, differential calculus, and optimization*, Adv. Des. Control, SIAM, Philadelphia, 2001.
[22] M. Delfour and J. Zolésio, *Shapes and Geometries: Metrics, Analysis, Differential Calculus and Optimization*, Adv. Des. Control, SIAM, Philadelphia, 2011.
[23] M. Delfour and J. Zolésio, *Shape derivatives for nonsmooth domains*, in Optimal Control of Partial Differential Equations, K.-H. Hoffmann and W. Krabs, eds., Lecture Notes in Control and Inform. Sci. 149, Springer, New York, 1991, pp. 38–55.
[24] C. Dorand, *Influence of Elliptical Distribution of Lift on Strength of Airplane Wings*, Technical memorandum, National Advisory Committee for Aeronautics, 1922.
[25] C. Eck, H. Garcke, and P. Knabner, *Mathematische Modellierung*, Springer, New York, 2008.
[26] L. Evans and R. Gariepy, *Measure Theory and Fine Properties of Functions*, Math. Chem. Ser., CRC Press, Boca Raton, FL, 1992.
[27] H. Garcke, *The* Γ*-limit of the Ginzburg-Landau energy in an elastic medium*, AMSA, 18 (2008), pp. 345–379.
[28] H. Garcke and C. Hecht, *A phase field approach for shape and topology optimization in Stokes flow*, New Trends in Shape Optimization, Internat Ser. Numer. Math., 166 (2015), pp. 103–116.
[29] H. Garcke and C. Hecht, *Shape and topology optimization in Stokes flow with a phase field approach*, Appl. Math. Optim., 73 (2016), pp. 23–70.
[30] E. Giusti, *Minimal Surfaces and Functions of Bounded Variation*, Notes Pure Math., Department of Pure Mathematics, Ann Arbor, MI, 1977.
[31] C. Hecht, *Shape and topology optimization in fluids using a phase field approach and an application in structural optimization*, Dissertation, University of Regensburg, Regensburg, Germany, 2014.
[32] F. Hettlich and W. Rundell, *The determination of a discontinuity in a conductivity from a single boundary measurement*, Inverse Problems, 14 (1998), pp. 67–82.
[33] A. Karchevsky, *Reconstruction of pressure velocities and boundaries of thin layers in thinly-stratified layers*, Inverse Ill-Posed Probl. Ser., 18 (2010), pp. 371–388.
[34] A. G. M. Michell, *The limits of economy of material in frame-structures*, Phil. Mag., 8 (1904), pp. 589–597.
[35] L. Modica, *The gradient theory of phase transitions and the minimal interface criterion*, Arch. Ration. Mech. Anal., 98 (1987), pp. 123–142.
[36] L. Modica and S. Mortola, *Un esempio di* Γ*-convergenza*, Boll. Unione Mat. Ital. B (5), 14 (1977), pp. 285–299.

[37] O. Pantz, *Sensibilité de l'équation de la chaleur aux sauts de conductivité*, C. R. Acad. Sci. Paris Ser. I, 34 (2005), pp. 333–337.

[38] P. Penzler, M. Rumpf, and B. Wirth, *A phase-field model for compliance shape optimization in nonlinear elasticity*, ESAIM Control Optim. Calc. Var., 18 (2012), pp. 229–258.

[39] D. Sale, A. Aliseda, M. Motley, and Y. Li, *Structural optimization of composite blades for wind and hydrokinetic turbines*, in Proceedings of the 1st Marine Energy Technology Symposium (METS 2013), 2013.

[40] R. Showalter, *Monotone Operators in Banach Spaces and Nonlinear Partial Differential Equations*, Math. Surveys Monogr. 49, AMS, Providence, RI, 1997.

[41] J. Simon, *Domain variation for drag in Stokes flow*, in Control Theory of Distributed Parameter Systems and Applications, Lecture Notes in Control and Inform. Sci. 159, 1991, pp. 28–42.

[42] K. Sturm, M. Hintermüller, and D. Hömberg, *Distortion compensation as a shape optimization problem for a sharp interface model*, Comput. Optim. Appl., 64 (2016), pp. 557–588, http://dx.doi.org/10.1007/s10589-015-9816-7.

[43] J. Thomsen, *Topology Optimization of Structures Composed of One or Two Materials*, Struct. Optim., 5 (1992), pp. 108–115.